

See discussions, stats, and author profiles for this publication at: <https://www.researchgate.net/publication/241091270>

Post-orogenic extension in the eastern part of the Jiangnan orogen: Evidence from ca 800–760 Ma volcanic rocks

Article in *Precambrian Research* · May 2014

DOI: 10.1016/j.precamres.2011.07.003

CITATIONS

78

READS

206

8 authors, including:



Xiao-Lei Wang

Nanjing University

49 PUBLICATIONS 1,467 CITATIONS

[SEE PROFILE](#)



Ming Tang

Rice University

13 PUBLICATIONS 168 CITATIONS

[SEE PROFILE](#)



Liang Qi

Chengdu University of Technology

108 PUBLICATIONS 2,468 CITATIONS

[SEE PROFILE](#)



Post-orogenic extension in the eastern part of the Jiangnan orogen: Evidence from *ca* 800–760 Ma volcanic rocks

Xiao-Lei Wang^{a,*}, Liang-Shu Shu^a, Guang-Fu Xing^b, Jin-Cheng Zhou^a, Ming Tang^a, Xu-Jie Shu^a, Liang Qi^c, Yan-Hua Hu^d

^a State Key Laboratory for Mineral Deposits Research, Department of Earth Sciences, Nanjing University, 22 Hankou Road, Nanjing, Jiangsu Province 210093, PR China

^b Nanjing Institute of Geology and Mineral Resources, Nanjing 210016, PR China

^c State Key Lab of Ore Deposit Geochemistry, Institute of Geochemistry, Chinese Academy of Sciences, Guiyang 550002, PR China

^d Zhejiang Institute of Geological Survey, Hangzhou 311203, PR China

ARTICLE INFO

Article history:

Received 27 February 2011

Received in revised form 28 June 2011

Accepted 2 July 2011

Available online 14 July 2011

Key words:

Post-orogenic
Extension
Neoproterozoic
Jiangnan orogen
Tectonic evolution
South China

ABSTRACT

We present a systematic geochronological and geochemical study on *ca* 800–760 Ma volcanic rocks in the eastern part of the Jiangnan orogen. The Xucun composite dykes are dated at *ca* 805 Ma; the mafic components have OIB-like trace-element patterns and positive anomalies in Zr and Hf. The least-contaminated sample has relatively depleted Nd isotopic features, suggesting the Xucun mafic dykes may have been generated from the partial melting of OIB-like asthenosphere with later crustal contamination. The Xucun felsic dykes have decoupled Nd–Hf isotopes, and the Hf-isotope compositions of zircons indicate that the dykes may be derived from the partial melting of the early Neoproterozoic juvenile crustal materials, with minor incorporation of Paleoproterozoic crustal components. The *ca* 800–790 Ma Shangshu volcanics include two compositional series: calc-alkaline and tholeiitic. The Shangshu calc-alkaline volcanics in the Minjiawu area have low abundances of LILE, HFSE and high Na₂O contents and Sr/Y ratios, similar to adakitic rocks. The evident arc-like geochemical features and radiogenic Nd isotopes ($\varepsilon_{\text{Nd}}(t)$) values of +3.7 to +4.8 suggest that these rocks may have been generated from the partial melting of juvenile lithospheric mantle metasomatized by Na-rich melts released from the subducted slab. The tholeiitic mafic rocks from the Shangshu bimodal volcanics represent two different magma sources. The partial melting of metasomatized lithospheric mantle led to the formation of arc-like basalts with low TiO₂ contents, negative anomalies in Zr and Hf, and high values of Mg[#] and $\varepsilon_{\text{Nd}}(t)$ (+6.2), whereas the partial melting of asthenospheric mantle generated volcanic rocks with high TiO₂ contents and low positive $\varepsilon_{\text{Nd}}(t)$ (+1.4 to +2.7), without negative anomalies of Nb, Ta, Zr and Hf. The Shangshu felsic rocks were formed by the reworking of early Neoproterozoic juvenile arc crustal materials. The *ca* 760 Ma mafic rocks from the Puling bimodal volcanics generally have low TiO₂ contents (<0.9 wt%), nearly flat REE distributions and arc-like trace-element patterns. They may have been generated from the high-degree partial melting of metasomatized lithospheric mantle. One sample has a high TiO₂ content (2.41 wt%) and high $\varepsilon_{\text{Nd}}(t)$ (+6.2), with overall OIB-like trace-element patterns, implying the local partial melting of asthenospheric mantle. The occurrence of significant volumes of bimodal volcanics in the eastern part of the Jiangnan orogen suggests an extensional setting in the period *ca* 800–760 Ma. The evident partial melting of newly-metasomatized lithospheric mantle and subordinate partial melting of asthenosphere suggest that post-orogenic extension shortly after the Neoproterozoic orogenesis may be a better explanation for the genesis of the mid-Neoproterozoic magmatic rocks in the eastern part of the Jiangnan orogen. Post-orogenic extension may be diachronous along the whole orogenic belt, and probably has no direct relationship with the Rodinia rifting event. A more detailed model is presented to illustrate the evolution of the eastern part of the Jiangnan orogen.

© 2011 Elsevier B.V. All rights reserved.

1. Introduction

The term 'orogeny', which was originally defined as a period of mountain building (Gilbert, 1890), has several meanings when applied to magmatism along continental margins. The evolution of an orogen, commonly termed as the Wilson cycle (Wilson,

* Corresponding author. Tel.: +86 25 83686336; fax: +86 25 83686016.
E-mail address: xlwangnju@yahoo.com.cn (X.-L. Wang).

1966), generally shows a progression from the opening of a new ocean, through plate subduction, to collision, and is recorded by metamorphism, deformation, arc and syn-collisional magmatism, angular unconformities, and post-orogenic extension. Some orogens that show no evidence of collision have been described as accretionary orogens (Collins, 2002). In the continental margins of paleo-continents or blocks, the identification of an orogenic belt and the reconstruction of its evolution always seem to be difficult (Burg and Ford, 1997). One especially controversial issue is the distinction between the transition from orogenic relaxation at post-collisional stages and back-arc areas to post-orogenic within-plate rifting (e.g., Bonin, 2004; Hyndman et al., 2005). In orogens that do not have enough diagnostic features in their regional metamorphism and deformation, magmatism and especially magmatic associations may become the most important factor in studying the orogenic evolution. Because the interpretations of geochemical data from magmatic rocks in orogenic belts are not always unique and unambiguous (e.g., Li et al., 2007; Wang et al., 2010a), it is necessary to combine the characteristics of magmatic associations and the whole evolutionary framework to define the tectonic settings at a given point in time.

The Jiangnan orogen, located between the Yangtze and Cathaysia blocks (Fig. 1a), was formed during early to middle Neoproterozoic time due to the assembly of the two blocks (Zhou and Zhu, 1993; Charvet et al., 1996; Zhao and Cawood, 1999; Zhou et al., 2004; Wang et al., 2007, 2010b, 2010c). The final amalgamation led to the formation of the South China Block (SCB) in Neoproterozoic time ($\text{ca } 860\text{--}820 \text{ Ma}$; Wang et al., 2007), although there was probably a failed rift approximately along the orogenic belt following the collision (Li et al., 1995). The extent and process of this assembly undoubtedly played a role in the generation of the abundant Phanerozoic magmatic rocks in the SCB. Therefore, the formation and evolution of the Jiangnan orogen have become a key issue in understanding the geology of the SCB.

The tectonic processes that built this orogen have been discussed for over three decades since Guo et al. (1977) proposed the 'trench-arc-basin system' model. It has been generally accepted that the orogen formed by the late Mesoproterozoic to early Neoproterozoic collision between the Yangtze and Cathaysia blocks (e.g., Bai et al., 1986; Shui et al., 1986; Chen et al., 1991; Cheng, 1991; Zhou and Zhu, 1993; Shu and Charvet, 1996; Charvet et al., 1996). The geological evidence for this orogenesis includes the presence of ophiolites, high-pressure blueschists, island-arc volcanic rocks, deformation and angular unconformities in the Jiangnan orogen.

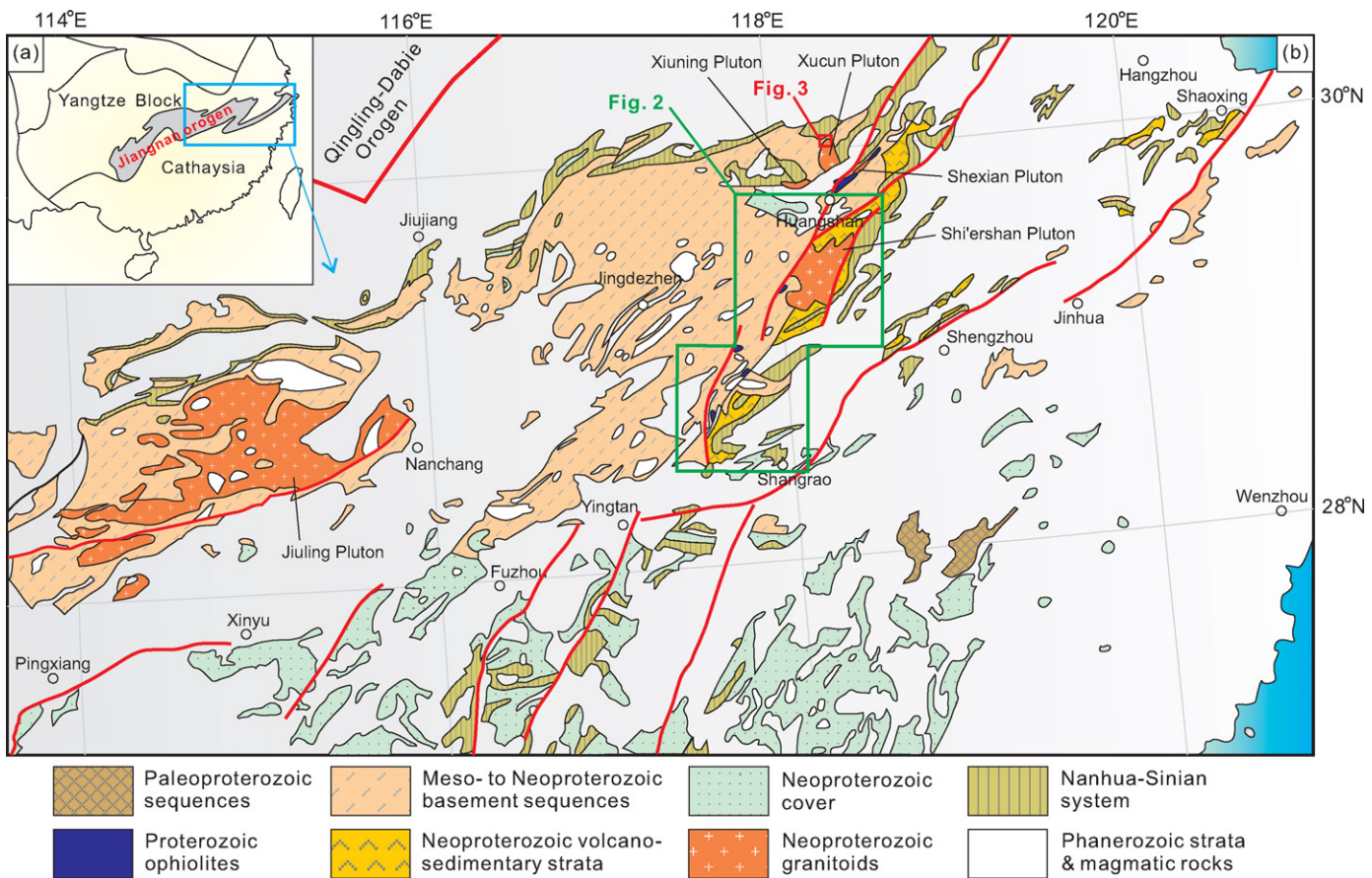
Early, less reliable dating results suggested that the Jiangnan orogen could be correlated with the Rodinia supercontinent that was mainly formed by Grenvillian-age orogenesis. However, more recent work dates the final amalgamation of the Yangtze and Cathaysia blocks to later than $\text{ca } 860 \text{ Ma}$, based on detrital zircon data for basement sequences (Wang et al., 2007; Zhou et al., 2009). The position of the SCB in Rodinia and the tectonic settings of Neoproterozoic magmatism in the Jiangnan orogen have become hotly-debated issues in the last decade, represented by three main models. The 'plume' model (Li et al., 1999, 2003a,b, 2008a,b) suggests that the $\text{ca } 850\text{--}750 \text{ Ma}$ magmatism in the Jiangnan orogen was related to a mantle (super-) plume and placed the SCB in the interior of Rodinia, between the eastern part of Australia and the southwestern part of Laurentia. However, the 'slab-arc' model (Zhou et al., 2002, 2004, 2009; Wang et al., 2004, 2006, 2007, 2008a; Yu et al., 2008) argues that the orogen was not directly connected to the main body of Rodinia, but existed as an isolated block, close to Australia and India, and considered the Neoproterozoic magmatic rocks as the products of subduction orogenesis. The 'plate-rift' model (Zheng et al., 2008) emphasizes the partial melting of different source materials during the tectonic collapse of an arc-continent collisional orogen. To test these different models, it

is essential to carry out detailed geological, structural and petrological investigations and more precise dating and comprehensive geochemical work are necessary. In this study, we present new LA-ICP-MS zircon data and geochemical data for the $\text{ca } 800\text{--}760 \text{ Ma}$ volcanic rocks in the eastern part of the Jiangnan orogen, which provide important insights into the tectonic evolution of the orogen.

2. Geological background

As a major block in East Asia, the South China Block (SCB) is separated from the North China Craton by the Qinling-Dabie orogen and from Tibet to the west by the Songpan-Ganze belt and Panxi Belt (Fig. 1a). The nearly W-E trending $\text{ca } 1500 \text{ km}$ Jiangnan orogen is located in the middle of the SCB, and divides it into two blocks: the Yangtze Block to the northwest and the Cathaysia Block to the southeast (Fig. 1a). Mesozoic granitoids and late Neoproterozoic strata are widespread in the Cathaysia Block (Zhou et al., 2006a), with a very few Paleoproterozoic sequences and magmatic rocks preserved in southern Zhejiang Province (Yu et al., 2009, 2010). The Yangtze Block has a late Archean continental nucleus in the Kongling area, and is surrounded by the Meso- to Neoproterozoic strata and magmatic rocks (Zhao et al., 2010). The Jiangnan orogen can be basically divided into two parts: (1) the western part is mainly distributed in western and northern Hunan Province, northeastern Guizhou Province and northern Guangxi Province (Zhou et al., 2004, 2009; Wang et al., 2004, 2006); (2) the eastern part covers western, northern and northeastern Jiangxi Province, southern Anhui Province, and northwestern Zhejiang Province (Zhou and Zhu, 1993; Shu and Charvet, 1996). Several types of orogenesis-related geological evidence are preserved in the eastern part of the Jiangnan orogen, including the $\text{ca } 1.0\text{--}0.96 \text{ Ga}$ ophiolites (Cheng, 1991; Zhou and Zhu, 1993), $\text{ca } 930\text{--}880 \text{ Ma}$ arc volcanic rocks and syn-collisional magmatic rocks in the Shuangxiwu area near Shaoxing city (Cheng, 1991; Li et al., 2009; Fig. 1b), and $866 \pm 14 \text{ Ma}$ high-pressure blueschists in northeastern (NE) Jiangxi Province (Charvet et al., 1996). Two major faults, the Jiangshan-Shaoxing Fault and the NE-trending Jiangxi Fault mark the southeastern margin of the Jiangnan orogen (Fig. 1b), with the former being the main boundary between the Yangtze and Cathaysia blocks (Zhou, 2003).

Magmatism in the eastern part of the Jiangnan orogen is dominated by Neoproterozoic granitic rocks, as indicated in Fig. 1b. The $\text{ca } 820 \text{ Ma}$ granitoids, including the Jiuling, Xucun, Xiuning and Shexian plutons (Fig. 1b), have received considerable attention in recent years (e.g., Zhou and Wang, 1988; Li et al., 2003a; Zheng et al., 2007). These granitic rocks intrude the Shuangqiaoshan Group, which is regarded as the basement sequence in the areas of Jiangxi and southern Anhui Provinces (Fig. 1b). These sedimentary sequences previously were considered to be of Mesoproterozoic age, but newly published zircon U-Pb dating results for the interlayered volcanic rocks and the adjacent similar sequences suggest that they are most likely to have formed in the period $870\text{--}820 \text{ Ma}$ (Wang et al., 2007, 2008b). The Shuangqiaoshan Group is unconformably overlain by Neoproterozoic volcano-sedimentary sequences, including the Luojiamen, Hongchicun and Shangshu Formations, from bottom to top (Fig. 2; Wang and Li, 2003). The Luojiamen Formation is composed mainly of conglomerates, sandstones and turbidites. It unconformably overlies the arc-related Shuangxiwu Group in northern Zhejiang Province, representing a foreland basin in the area (Cheng, 1991). The Hongchicun Formation is composed of purple conglomerates, sandstones (Cheng, 1991) and few volcanic rocks with zircon SHRIMP U-Pb age of $797 \pm 11 \text{ Ma}$ (Li et al., 2003b). The Shangshu Formation dominates the Neoproterozoic cover in the eastern part of the Jiangnan orogen, and comprises at least two stages of volcanic eruption, with



basalts, basaltic andesites, andesites, dacites, rhyolites and tuffs (Fig. 2; Shu et al., 1995). This formation is mainly distributed along the Jiangshan-Shaoxing Fault in northern Zhejiang Province and the NE Jiangxi Fault in southern Anhui Province and northeastern Jiangxi Province (Fig. 1b). The Shangshu volcanic rocks in turn were intruded by the 779 ± 11 Ma Shi'ershan granites in southern Anhui (Li et al., 2003b). Li et al. (2008b) gave a zircon SHRIMP U-Pb age of 792 ± 5 Ma for the Shangshu rhyolites in northern Zhejiang. Zheng et al. (2008) found two age groups in zircons from the Shangshu Formation in southern Anhui, and interpreted the ages of 779 ± 7 Ma and 773 ± 7 Ma as the timing of the eruption. Nearly contemporaneous with the Shangshu Formation and the Shi'ershan granites was the emplacement of the A2-type Daolinshan granites that intrude the Shuangxiwu Group, with published ages of 794 ± 9 Ma (Li et al., 2008b) and ca 780 Ma (Wang et al., 2010b). They show bimodal features with associated mafic dykes (Li et al., 2008b).

Similar bimodal mafic-felsic dykes occur in Xucun and Puling Villages, southern Anhui. The Xucun composite dykes cut the northern part of the ca 820 Ma Xucun Pluton (Tang et al., 1997), but their ages and tectonic settings remain unclear. They are composed of over twenty parallel dykes, generally showing NE-stretching, with widths about 2–7 m for individual dykes (Tang et al., 1997). Diabase and granitic porphyry are the two distinctive rock types in the composite dykes. The Puling Formation, which was previously considered basically equivalent to the upper part of the Shangshu Formation (BGMRAP, 1987), is unconformably overlain by the Sinian Xuning Formation (Ma et al., 2001). It is composed of andesites and tuffs, and lesser tuffaceous sandstones (BGMRAP, 1987). Ma et al. (2001) proposed that the main rock types of the formation are basalts, basaltic andesites, tuffs, and sandstones, formed

in an extensional (rift) setting. This formation also lacks precise dating constraints. In this study, we investigated typical profile of the Puling Formation near the Tuanjie Village, southern Anhui Province, and found that it is in fact composed of bimodal volcanic rocks, including basalts, rhyolites and few tuffs. After the deposition of the Xuning Formation, there was no evident Precambrian magmatic activity in the eastern part of the Jiangnan orogen.

Here we present chronological and detailed geochemical data for the volcanic rocks of the Shangshu Formation the Xucun composite dykes and the Puling Formation. On the basis of these new data, we present an alternative evolution model for the tectonic evolution of the eastern part of the Jiangnan orogen during Neoproterozoic time.

3. Petrography

3.1. Xucun composite dykes

The compositions of individual dykes in the Xucun area can be mafic, felsic or intermediate. Most of the plagioclase in the diabases is replaced by calcite, although they generally keep their prismatic shapes. Most of the pyroxene has been replaced by chlorite and magnetite. Some samples show a porphyritic texture, with phenocrysts of pyroxene and plagioclase ($An = 42–50$; Tang et al., 1997). A few quartz grains are surrounded by pyroxene due to disequilibrium reactions, suggesting that they may have been captured from the granitic porphyry.

The granite porphyries are relatively fresh, although the replacements by calcite, chlorite and sericite can also be found in these rocks. The phenocrysts are composed of β -quartz and plagioclase

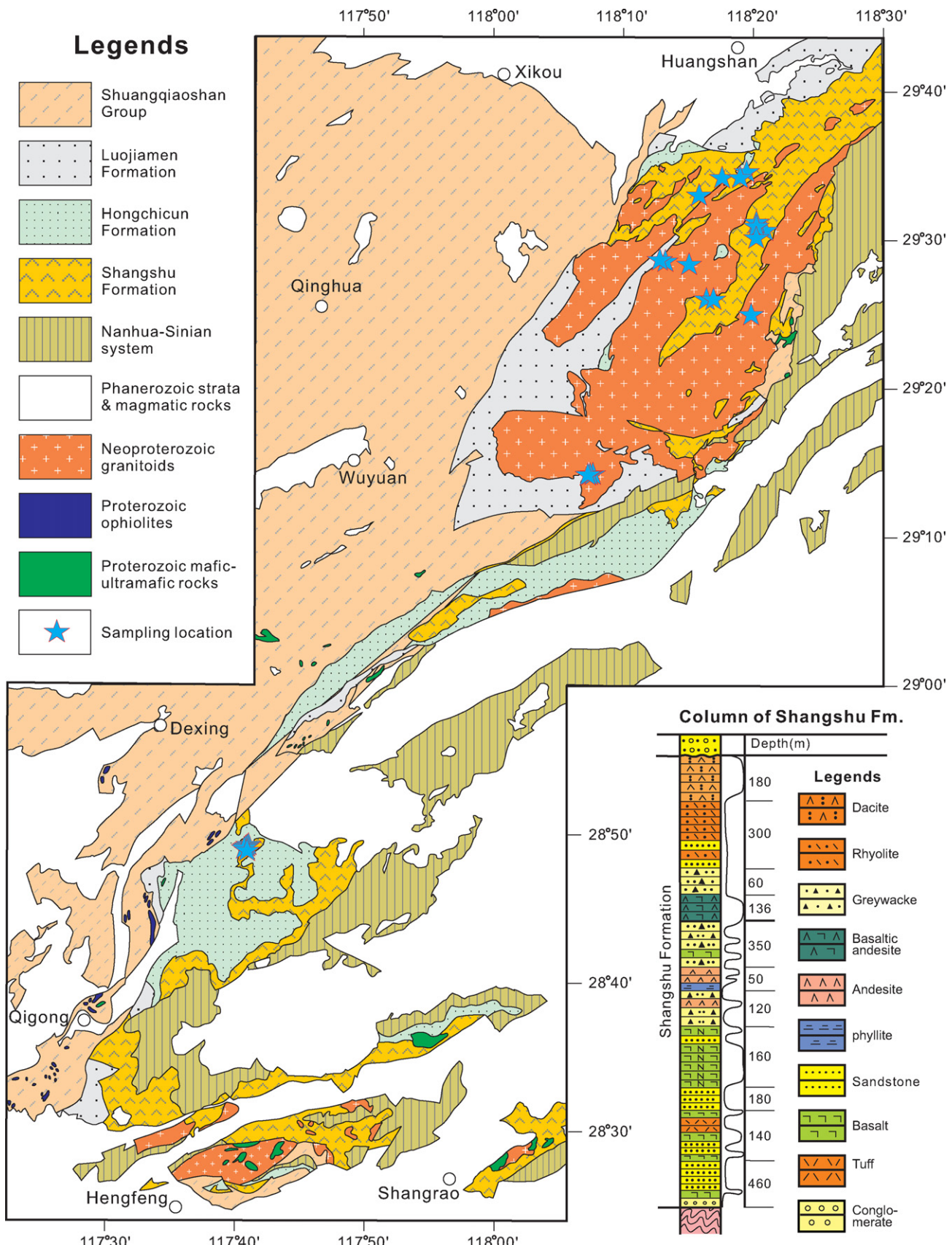


Fig. 2. Geological map showing the distribution of the Shangshu Formation in the eastern part of the Jiangnan orogen (modified after JPIGS, 2006, 2007). The lower right inset is the stratigraphic column of the Shangshu Formation.

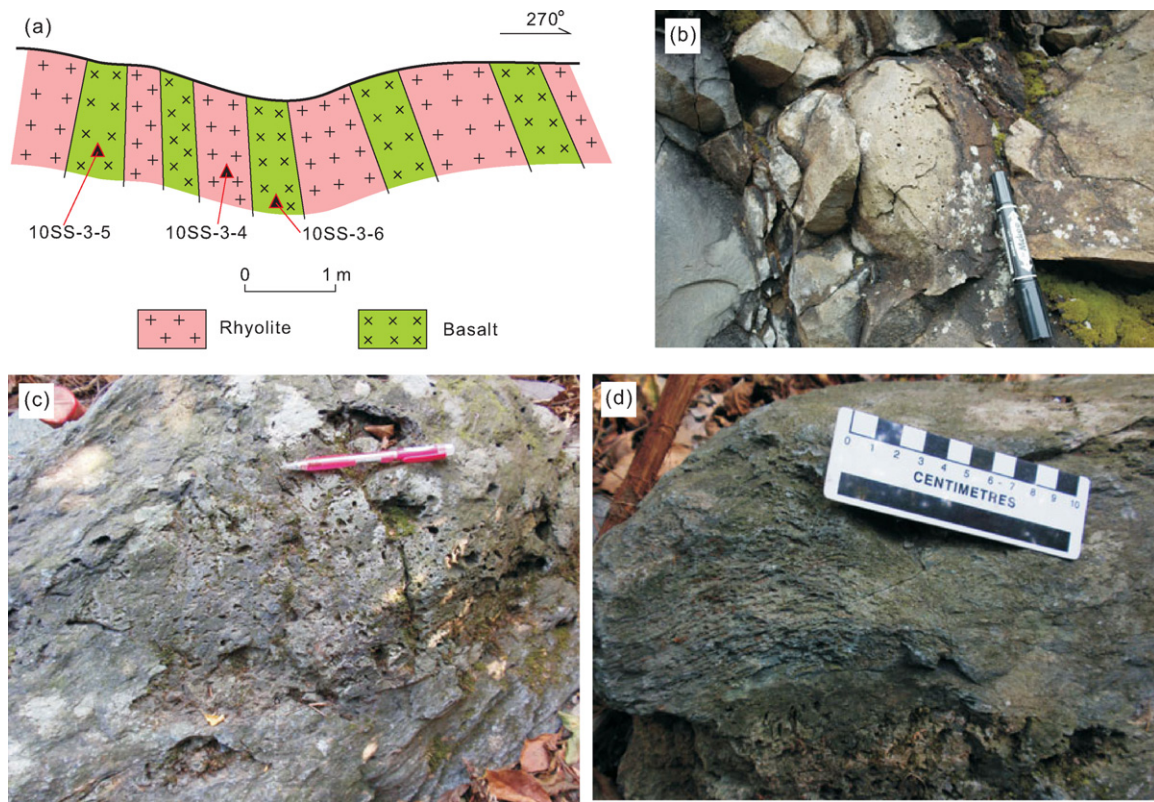


Fig. 3. Field pictures of the Shangshu and Puling bimodal volcanics. (a) Field drawing of the Shangshu bimodal volcanics. (b) Field photo of the Shangshu pillowved basalt with vesicular structure. (c) Field photo showing the vesicular structure in the Puling basalts. (d) The elongate vesicular structure in the Puling basalts.

($An = 25\text{--}30$). Embayments are generally developed at the margins of the β -quartz, which may have resulted from shrinking during the phase transition to α -quartz. In addition, needle-like apatite is generally present in the granitic rocks, suggesting a rapid eruption process.

3.2. Shangshu formation

The Shangshu volcanic rocks were collected from southern Anhui and northwestern Zhejiang Provinces, around the Shi'ershan granite pluton. The volcanic rocks in the Minjiawu area of northeastern Jiangxi Province are composed of mafic and intermediate rocks, lacking felsic rocks. The other mafic rocks of the Shangshu Formation generally show a bimodal distribution of compositions (Fig. 3a). As presented in the following section, the two series show different geochemical characteristics. Therefore, we have separated these rocks into two subgroups in the discussion section: the Minjiawu volcanics and the Shangshu bimodal volcanics. Some of the basalts of the Shangshu bimodal volcanics show pillowved and vesicular structures (Fig. 3b). Mafic minerals of the rocks are replaced by chlorite, calcite, epidote, and magnetite. Plagioclase ($An = 53\text{--}62$) is relatively fresh and shows a preferred orientation, suggesting an eruptive feature. The volcanics in the Minjiawu area are relatively fresh, and show a distinct preferred orientation, suggesting magma flowage. Plagioclase ($An = 26\text{--}32$) and pyroxene are the dominant phenocrysts in these volcanics. Tiny fresh hornblendes are preserved, whereas pyroxenes are replaced by calcite.

The rhyolites from the Shangshu bimodal volcanics are relatively fresh. K-feldspar is the dominate phenocryst, with minor plagioclase and quartz. The twins of plagioclase are generally bent, suggesting the effect of later stress. The re-crystallization of quartz is evident in many samples, suggesting that the Shangshu volcanics experienced low-grade metamorphism similar to Neoproterozoic

detrital sedimentary rocks in the eastern part of the Jiangnan orogen.

3.3. Puling formation

The volcanic rocks of the Puling Formation show different colors in the field, with caesious basalts, purple rhyolites and off-white tuffs. A vesicular structure is widely developed in the basalts (Fig. 3c), and vesicles show flattened and elongate shapes (Fig. 3d), suggesting the flow of magma. Some of the vesicles are filled with calcite. The vesicular structure in sample 09WN-2-7 is not as marked as in the other samples, and prismatic plagioclases ($An = 41\text{--}50$) in the sample do not show preferred orientation. The rhyolites and tuffs of the Puling Formation are not very fresh, due to reworking by later tectonic processes; this has produced a schistosity defined by orientated tiny flakes of muscovite. Quartz is the main phenocryst in the rhyolites.

4. Analytical methods

Representative samples were selected for zircon U-Pb dating; the isotopic results are listed in Table 1. Zircons were separated using conventional heavy liquid and magnetic techniques, mounted in epoxy resin and polished down. Cathodo-luminescence (CL) images of zircons were acquired at the State Key Laboratory of Continental Dynamics, Northwest University (NWU), Xi'an. LA-ICP-MS zircon U-Pb dating was carried out at the State Key Laboratory for Mineral Deposits Research (MiDeR), Nanjing University (NJU), using an Agilent 7500a ICP-MS attached to a New Wave 213 nm laser ablation system. All of the spot analyses were carried out using a beam with a ca 25 μm diameter and a repetition rate of 5 Hz and 70% energy. Detailed analytical procedures and data acquisition are similar to those described by Wang et al. (2007).

Major-element compositions of the samples were analyzed using an ICP-AES (JY38S) at the MiDeR, NJU, with analytical precision generally better than 2% (RSD). Trace elements in the Xucun composite dykes were analyzed using ICP-MS (Finnigan MAT-Element 2) techniques at the MiDeR, NJU. The Puling bimodal volcanics and some samples from the Shangshu Formation were analyzed using ICP-MS (Finnigan MAT-Element) at the Institute of Geochemistry Chinese Academy of Sciences, Guiyang. Analytical precision for most elements analyzed by the Element instruments is better than 5%. The remaining samples were analyzed using ICP-MS (PerkinElmer) at ALS Chemex, Guangzhou. Analytical precision for most elements is better than 10%. Sr–Nd isotopes were analyzed using ID-TIMS (Finnigan MAT Triton TI) at the MiDeR, NJU. Chemical separation procedures are similar to those described by [Pu et al. \(2005\)](#), with relative standard deviation (RSD) lower than 5×10^{-6} . Mass fractionation was corrected assuming $^{86}\text{Sr}/^{88}\text{Sr} = 0.1194$. Mass fractionation of Nd isotopes was corrected assuming $^{146}\text{Nd}/^{144}\text{Nd} = 0.7219$. The $\varepsilon_{\text{Nd}}(t)$ values were calculated based on the Nd isotopic compositions of $^{143}\text{Nd}/^{144}\text{Nd}$ (CHUR) = 0.512638 and $^{147}\text{Sm}/^{144}\text{Nd}$ (CHUR) = 0.1967.

Zircon Lu–Hf analyses were carried out *in situ* using a Geolas CQ 193 nm ArF excimer laser ablation system at the Institute of Geology and Geophysics, CAS. The analytical techniques are similar to those described in detail by [Wu et al. \(2006a\)](#). All analyses were carried out using a beam with a *ca* 40–50 μm diameter and a 6 Hz repetition rate. A new TIMS-determined value of 0.5887 for $^{176}\text{Yb}/^{172}\text{Yb}$ was applied for correction ([Vervoort et al., 2004](#)). The decay constant for ^{176}Lu of $1.865 \times 10^{-11} \text{ year}^{-1}$ proposed by [Scherer et al. \(2001\)](#) was adopted in this work. ε_{Hf} values were calculated according to the chondritic values of [Blichert-Toft et al. \(1997\)](#). Single-stage model ages (T_{DM1}) were calculated referred to the depleted mantle with a present-day $^{176}\text{Hf}/^{177}\text{Hf}$ ratio of 0.28325, similar to that of the average MORB ([Nowell et al., 1998](#)) and $^{176}\text{Lu}/^{177}\text{Hf}$ ratio of 0.0384 ([Griffin et al., 2000](#)). A “crustal” model ages (T_{DM2}) were also calculated by assuming the parent magma was produced from average continental crust ($^{176}\text{Lu}/^{177}\text{Hf} = 0.015$; [Griffin et al., 2000](#)) that originally was derived from the depleted mantle.

5. Dating results

5.1. Xucun composite dykes

Sample 07XC-1-5 (N30°01'41.1", E118°19'28.0") is a granite porphyry. Zircons from the sample are generally prismatic in shape with clear oscillatory zoning ([Fig. 4](#)). Th and U contents of the twenty dated zircons range between 28 and 405 ppm and 42–430 ppm, respectively, and Th/U ratios vary from 0.29 to 1.48. One analysis shows a relatively older $^{206}\text{Pb}/^{238}\text{U}$ age of 831 ± 9 Ma, which is identical with the crystallization age of the Xucun Pluton, suggesting that the zircon was captured from the wall rock. The remaining nineteen analyses yielded a weighted average $^{206}\text{Pb}/^{238}\text{U}$ age of 805 ± 4 Ma ([Fig. 5a](#); $n = 19$, MSWD = 0.54).

Sample 07XC-1-1 is a diabase collected from a site near sample 07XC-1-5. Ten zircons separated from the rock are generally tiny, with lengths of 50–80 μm and widths of 40–60 μm , and show faint broad oscillatory zoning ([Fig. 4](#)). Two zircons gave late-Mesoproterozoic ages (1108 ± 12 Ma and 1001 ± 12 Ma). One zircon is strongly discordant, with a $^{207}\text{Pb}/^{206}\text{Pb}$ age of 2469 ± 27 Ma ([Table 1](#); [Fig. 5b](#)). The remaining seven zircons fall into a group, yielding an upper intercept age of 807 ± 10 Ma and a weighted average $^{206}\text{Pb}/^{238}\text{U}$ age of 804 ± 7 Ma ([Fig. 5b](#); $n = 7$, MSWD = 0.64); the latter is considered to best represent the crystallization age of the diabases in the Xucun dykes.

Therefore, the mafic and felsic rocks from the Xucun composite dykes have identical U–Pb ages of *ca* 805 Ma, and the similarity of ages is also consistent with the field observations.

5.2. Shangshu formation

Sample 09JX-3-1 (N28°48'55.59", E117°42'26.47") is a basalt collected from the Shangshu Formation in the Minjiawu area, northeastern Jiangxi Province. Zircons generally show broad and bright oscillatory zoning ([Fig. 4](#)). Of 18 zircons, two yield Archean $^{207}\text{Pb}/^{206}\text{Pb}$ ages ([Table 1](#); 2591 ± 45 Ma and 2517 ± 40 Ma), and six give Paleoproterozoic $^{207}\text{Pb}/^{206}\text{Pb}$ ages ([Table 1](#)). The remaining nine analyses are identical within error, and yield a weighted average $^{206}\text{Pb}/^{238}\text{U}$ age of 802 ± 8 Ma ([Fig. 6a](#); $n = 9$, MSWD = 1.0).

Sample 10SS-4-2 (N29°31'27.69", E118°20'19.95") is a dacite from southern Anhui Province, adjacent to the Shi'ershan Pluton. Fifteen analyses have Th/U ratios ranging from 0.35 to 1.05. One spot analysis yields a $^{207}\text{Pb}/^{206}\text{Pb}$ age of 2412 ± 48 Ma; the other 14 analyses have identical ages, and yield a weighted average $^{206}\text{Pb}/^{238}\text{U}$ age of 794 ± 7 Ma ([Fig. 6b](#); $n = 14$, MSWD = 0.19).

Sample 10SS-16-1 (N29°14'49.98", E118°05'23.60") is a rhyolitic porphyry. Zircons from this sample have Th/U ratios of 0.75–1.11. Fourteen analyses from this sample fall in a group, yielding a weighted average $^{206}\text{Pb}/^{238}\text{U}$ age of 797 ± 6 Ma ([Fig. 6c](#); $n = 14$, MSWD = 0.18).

Sample SS-20 (N29°05'42.0", E118°03'32.4") is a rhyolite collected at the boundary between Jiangxi and Zhejiang Provinces. Nine spot analyses of zircons were obtained, with Th/U ratios from 0.49 to 0.73, and yield a weighted average $^{206}\text{Pb}/^{238}\text{U}$ age of 797 ± 5 Ma ([Fig. 6d](#); $n = 9$, MSWD = 0.17).

5.3. Puling formation

Three samples from the Puling Formation were dated. 09WN-1-1 (N29°58'15.25", E117°33'05.72") is a rhyolite sample, from which 15 zircons were analyzed. They generally have oscillatory zoning ([Fig. 4](#)), and their Th and U contents are relatively low, with the ranges of 11–245 ppm and 13–212 ppm, respectively. Th/U ratios range from 0.59 to 1.80. One analysis gives a Paleoproterozoic $^{207}\text{Pb}/^{206}\text{Pb}$ age of 2317 ± 67 Ma ([Table 1](#); [Fig. 7a](#)). The other 14 analyses are identical within error, yielding a weighted average $^{206}\text{Pb}/^{238}\text{U}$ age of 765 ± 7 Ma ($n = 14$, MSWD = 0.34).

Sample 09WN-4-1 (N29°58'16.36", E117°33'06.99") is a tuff. Zircons from the sample are tiny and also have clear oscillatory zoning ([Fig. 4](#)). Th/U ratios of the dated twenty-two zircons range from 0.64 to 3.4, except for one analysis (Th/U = 0.1) which has a $^{207}\text{Pb}/^{206}\text{Pb}$ age of 2048 ± 15 Ma. Although some analyses are not concordant, the $^{207}\text{Pb}/^{206}\text{Pb}$ ages show three peaks for inherited zircons: *ca* 2.6–2.4 Ga (five spots), *ca* 2.1–1.8 Ga (nine spots), and *ca* 1.05 Ga (two spots). The remaining six analyses yield a weighted average $^{206}\text{Pb}/^{238}\text{U}$ age of 751 ± 8 Ma ([Fig. 7b](#); $n = 6$, MSWD = 0.18).

Sample 09WN-6-1 (N29°58'23.63", E117°33'07.43") is also a tuff. Zircons from it are tiny and also have clear oscillatory zoning ([Fig. 4](#)). Th/U ratios of the dated 14 zircons range from 0.79 to 2.77. Two analyses show Paleoproterozoic (*ca* 2.0 Ga) ages, and one gives a late Mesoproterozoic age of 1008 ± 26 Ma. Six analyses have $^{206}\text{Pb}/^{238}\text{U}$ ages around 860–820 Ma, and the other five spot analyses yield a weighted average $^{206}\text{Pb}/^{238}\text{U}$ age of 763 ± 12 Ma ([Fig. 7c](#); $n = 5$, MSWD = 0.035).

Summarizing these data, we propose a mean age of *ca* 760 Ma as dating the eruption of the Puling volcanics. The tuffs have many inherited zircons, and their age peaks in Paleoproterozoic and late Archean time ([Fig. 7d](#)) are consistent with ages from the detrital zircons of the basement sequences ([Wang et al., 2007](#); [Zhou et al., 2009](#)). The ages of the Neoproterozoic inherited zircons ([Fig. 7c](#)) are basically coincident with the crystallization ages of the widespread

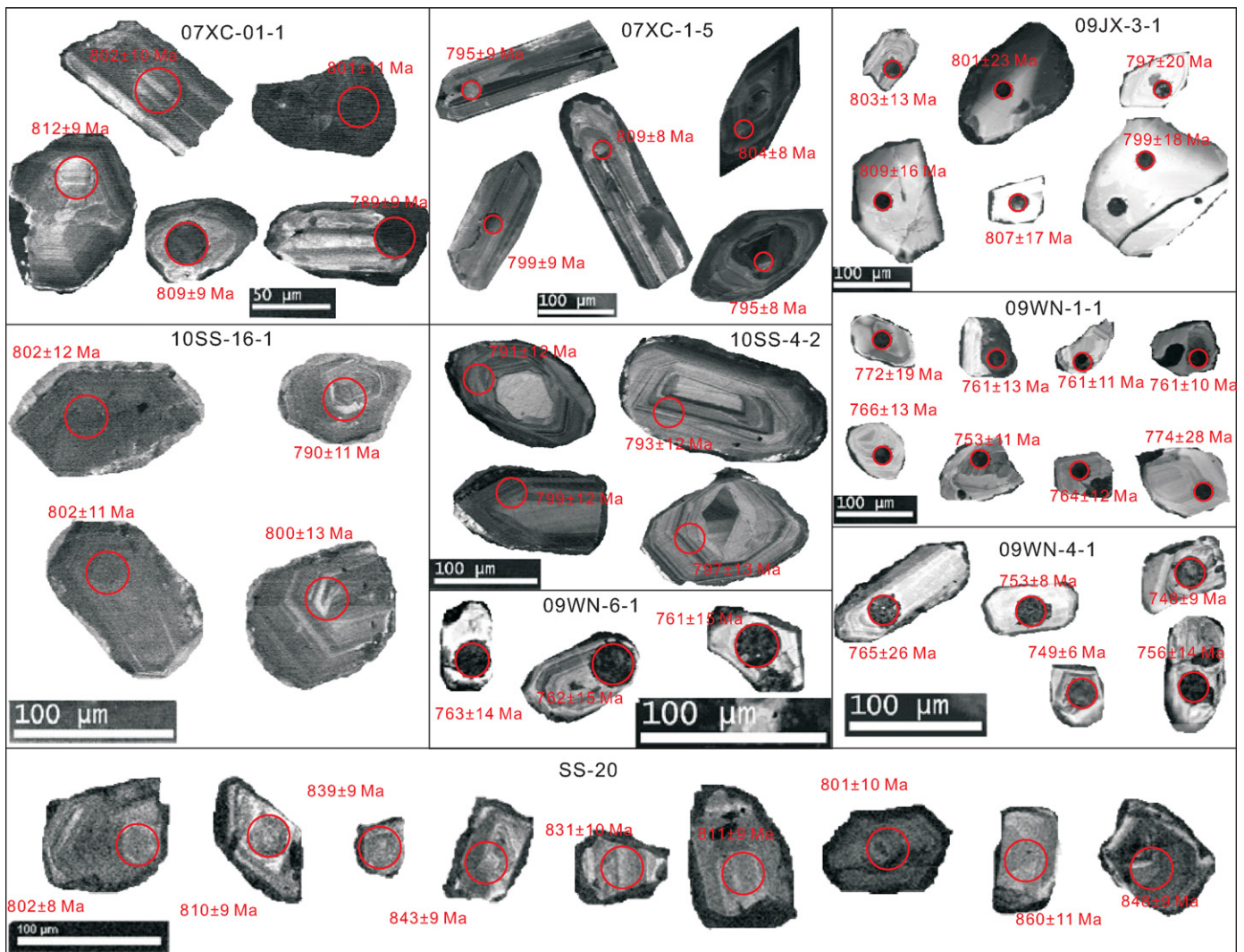


Fig. 4. Representative cathodo-luminescence (CL) images for analyzed zircons. The dating spots are denoted by the solid open circles with analyzed $^{206}\text{Pb}/^{238}\text{U}$ ages.

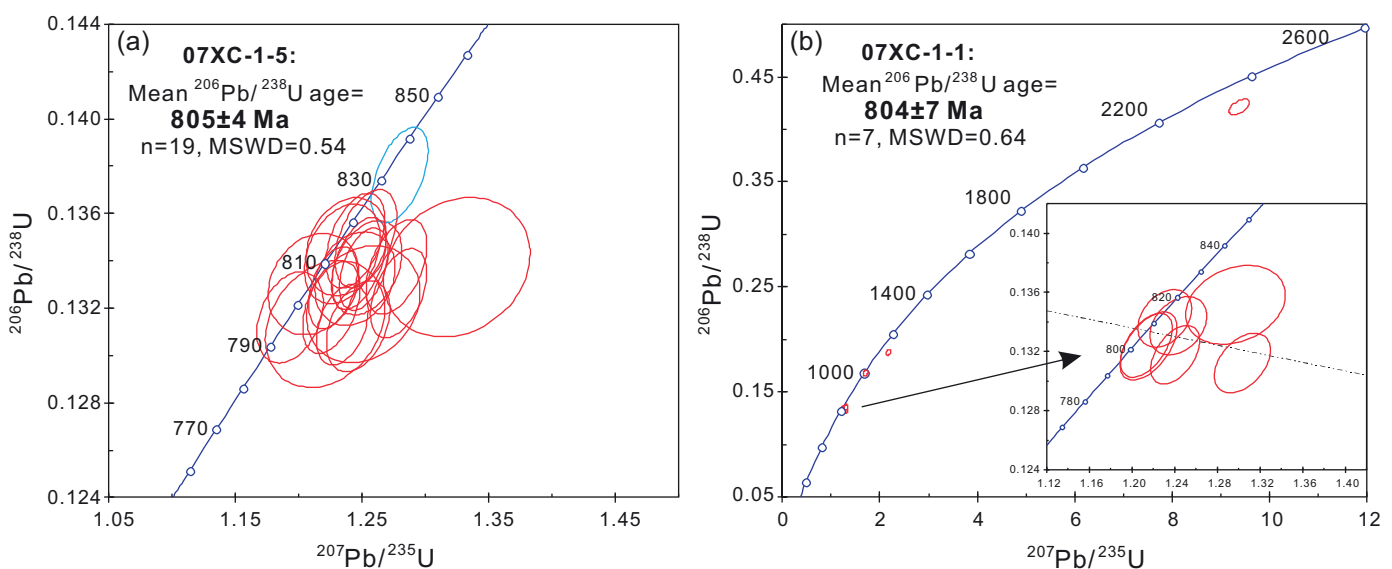


Fig. 5. Zircon U-Pb Concordia for the rocks of the Xucun composite dykes.

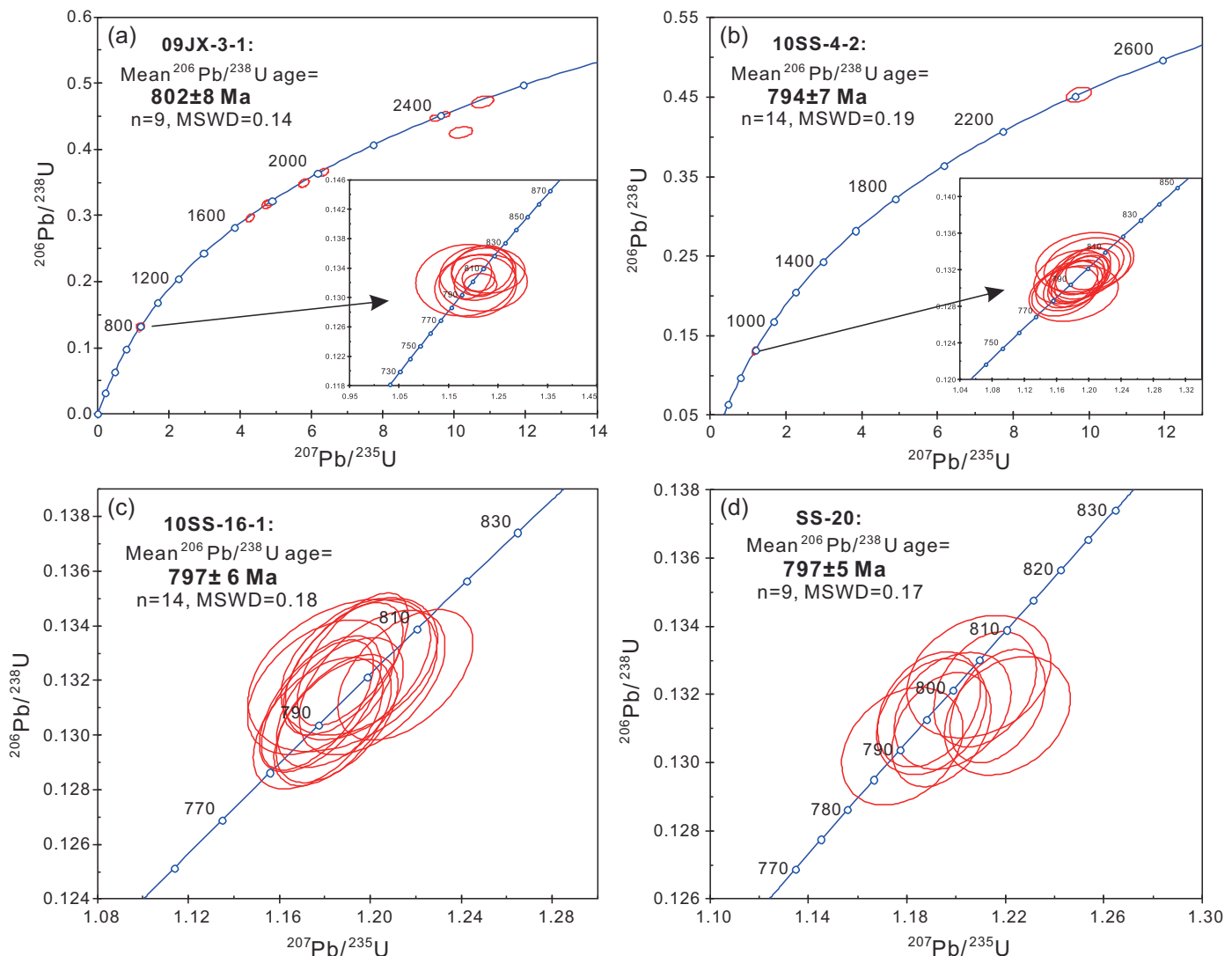


Fig. 6. Zircon U–Pb Concordia for the volcanic rocks of the Shangshu Formation.

Neoproterozoic granitoids in the Jiangnan orogen (e.g., Li et al., 2003a; Wang et al., 2006).

6. Geochemistry

6.1. Classification

Major-element and trace-element data are listed in Table 2. Because of high LOI contents in some samples, totals for major oxides of the mafic to intermediate rocks are recalculated to 100% (volatile free) for presentation in plots. On the alkali–SiO₂ diagram and Zr/TiO₂–Nb/Y diagram (Fig. 10a and b), most of the mafic rocks of this study classify as basalts and basaltic andesites, and the felsic rocks classify as rhyolites and dacites. A few samples of the Minjiawu volcanics are classified as andesite and dacites (Fig. 8b). The felsic rocks of this study are further classified as peraluminous, using the ACNK-ANK diagram (Fig. 8c). The tuffs and rhyolites of the Puling Formation are not shown in Fig. 8 because their high ASI (Aluminum saturation index) values are outside the scale. The felsic rocks fall within or close to the areas of I, M and S-type granites (Fig. 8d), distinguishing them from the published analyses of the Shangshu felsic volcanics (Li et al., 2008b) and Daolinshan granites

(Wang et al., 2010b) that are adjacent to the Jiangshan-Shaoxing Fault.

The volcanic rocks of this study are mainly classified as sub-alkaline in the alkali–SiO₂ and Zr/TiO₂–Nb/Y diagrams (Fig. 8a and b). In order to understand the attributes of the studied volcanic rocks, we use the AFM diagram to provide further classifications. The mafic to felsic rocks of the Xucun composite dykes show a clear calc-alkaline tendency, with a few samples plotting in the tholeiitic field (Fig. 9a). The Minjiawu volcanics also define a calc-alkaline tendency (Fig. 9b), while the Shangshu bimodal volcanic rocks basically have a tholeiitic trend (Fig. 9c), suggesting the complexity of magma sources of the Shangshu volcanics. The Puling volcanics, especially the mafic rocks, show a tholeiitic trend (Fig. 9d).

6.2. Xucun composite dykes

The granitic porphyries of the Xucun composite dykes have restricted SiO₂ contents, within the range of 68.06–70.12 wt%. The diabases have SiO₂ contents ranging from 50.0 to 54.8 wt% (Table 2). One sample (10WN-15-3) from the mafic dykes has an intermediate SiO₂ content of 61.5 wt%. TiO₂ contents of the diabases range from 1.17 to 2.17 wt%. The MgO contents are not high, within the range

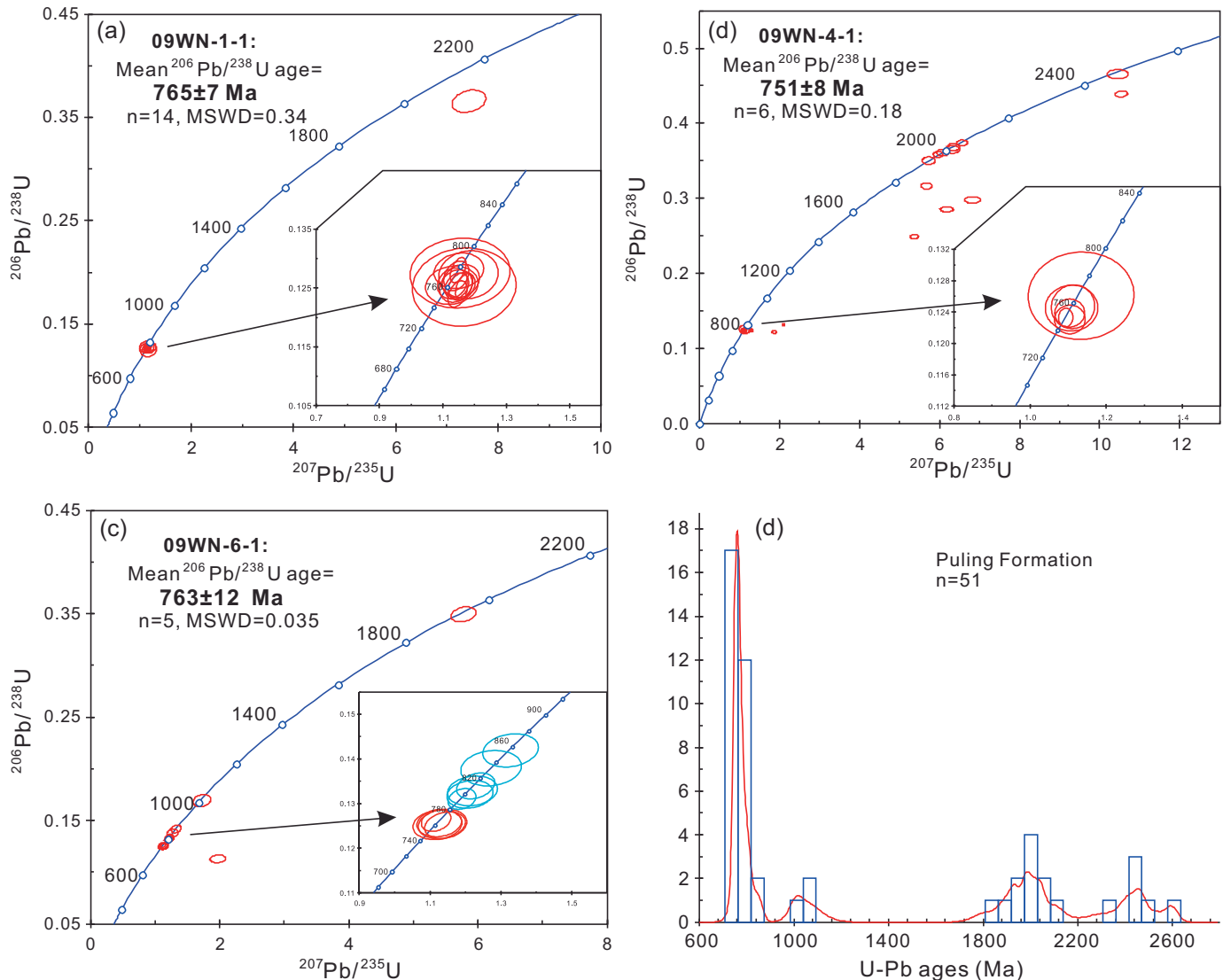


Fig. 7. Zircon U-Pb Concordia for the Puling bimodal volcanic rocks.

of 2.64–5.71 wt%, yielding fractionated Mg[#] of 27–51. Although the Na₂O contents of the mafic to intermediate rocks show rough positive correlations with the Mg[#], the K₂O contents are scattered, suggesting that the high Na₂O/K₂O ratios (1.09–3.62) of the mafic rocks may reflect the observed alteration.

The rocks from the Xucun composite dykes show similar distributions of rare earth elements (REE) and trace elements (Fig. 10), whether they are felsic or mafic in composition. Light REEs (LREE) are moderately enriched (Fig. 10a and c), with (La/Yb)_N values of 2.77–9.16 for mafic to intermediate rocks and of 5.84–8.30 for granitic porphyries (Table 2). The depletions in Nb and Ta are similar to those seen in average continental-arc basalts (Fig. 10b). However, the high LILE contents, the strongly positive Pb anomalies, the absence of positive Sr anomalies in most samples, and the positive anomalies in Zr and Hf (Fig. 10b) suggest that they were not generated from the metasomatized lithospheric mantle. Therefore, the negative anomalies of Nb and Ta may dominantly result from crustal contamination.

The rocks from the Xucun composite dykes have Nd-isotope compositions reflecting their LREE enrichment. Except for one sample (07XC-04-1, $\varepsilon_{\text{Nd}}(t) = -1.4$), the diabases and granitic porphyries have similar low $^{143}\text{Nd}/^{144}\text{Nd}$ ratios (from 0.512205 to 0.512356), giving low $\varepsilon_{\text{Nd}}(t)$ values of −5.5 to −8.4 (Table 3). The granitic

porphyries have similar Nd-isotope features to the diabases, with $\varepsilon_{\text{Nd}}(t)$ values of −7.4 to 8.4 vs −5.5 to −6.6.

The dated zircons were further analyzed for Lu–Hf isotopes (Table 4). Because the zircon grains are tiny, only seven Hf isotope spot analyses were obtained for zircons of the diabase. Two zircons with late Mesoproterozoic ages have $\varepsilon_{\text{Hf}}(t)$ values of −3.5 and −8.0, with calculated $T_{\text{DM}2}$ of 2167 ± 31 Ma and 2381 ± 39 Ma, respectively. The remaining five analyses with ages around ca 800 Ma have positive $\varepsilon_{\text{Hf}}(t)$. Among them, one analysis has the highest $\varepsilon_{\text{Hf}}(t)$ of +14.5, suggesting the presence of extremely depleted mantle components (high Lu/Hf) in the magma source. The other four analyses have $T_{\text{DM}1}$ from 1175 to 1240 Ma, very similar to the Hf isotopes of zircons from other Neoproterozoic granitoids in the eastern part of the Jiangnan orogen (Wu et al., 2006b; Zheng et al., 2007, 2008). Zircons from the granitic porphyry have similar Hf-isotope features, with a mean $\varepsilon_{\text{Hf}}(t)$ value of $+3.8 \pm 0.7$ ($n = 18$, 2σ , MSWD = 5.7) and a mean $T_{\text{DM}1}$ of 1222 ± 26 Ma ($n = 18$, 2σ , MSWD = 4.3), probably suggesting the reworking of juvenile arc-related crustal materials. One analysis has a negative $\varepsilon_{\text{Hf}}(t)$ of -4.11 ± 0.9 , indicating that old crustal components may have also been incorporated into the magma source. The Hf isotopes of the zircons are decoupled from the whole-rock Nd isotopes of the granitic porphyries ($\varepsilon_{\text{Nd}}(t) = -7.35$ to -8.45), which may be generated from the zircon

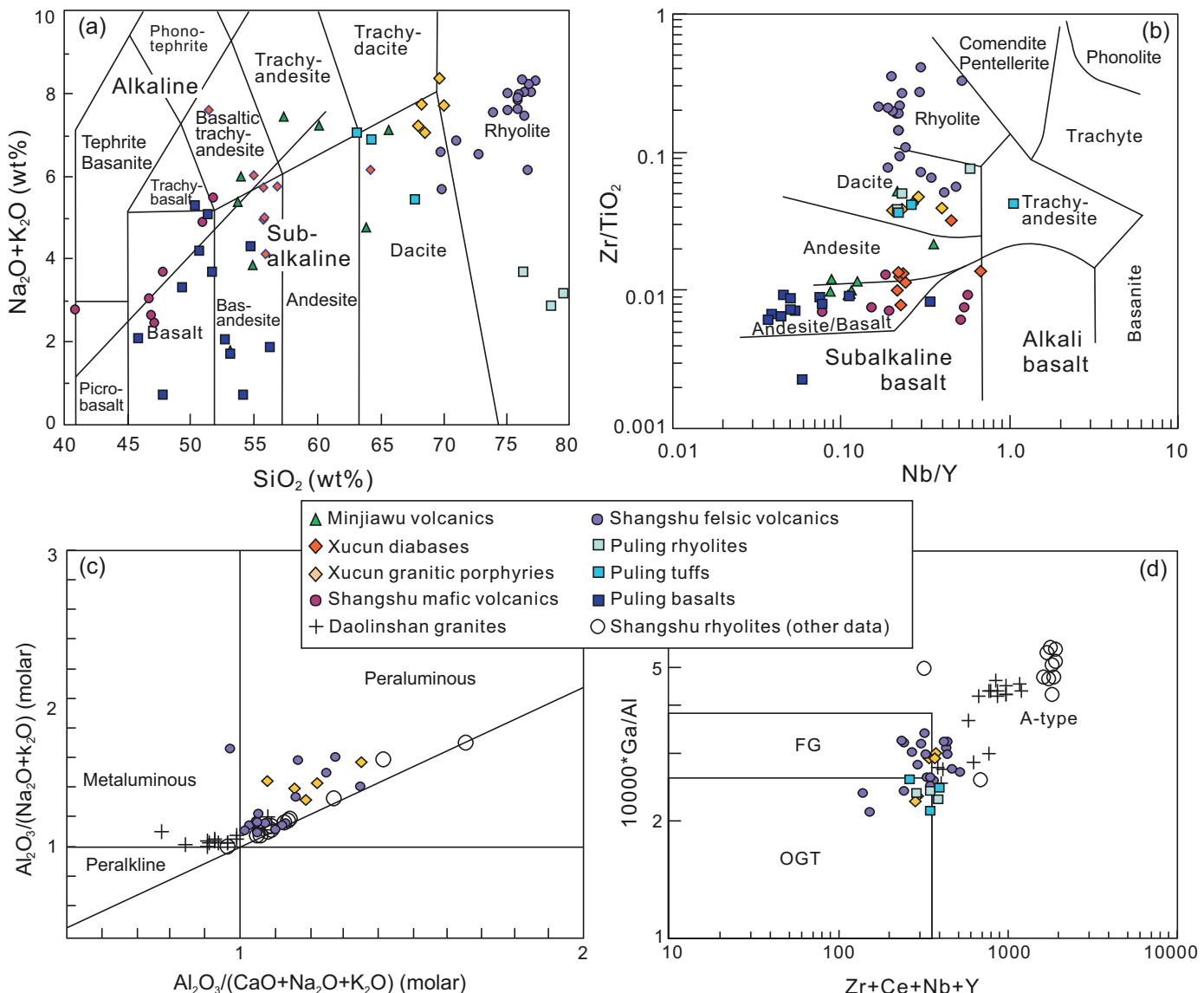


Fig. 8. Rock classification diagrams for the volcanic rocks in the eastern part of the Jiangnan orogen. (a) TAS diagram (after Maitre et al., 1989). (b) Zr/TiO_2 - Nb/Y diagram (after Winchester and Floyd, 1977). (c) ACNK-ANK diagram (after Maniar and Piccoli, 1989); (d) $10000 \times \text{Ga}/\text{Al}$ vs $(\text{Zr} + \text{Nb} + \text{Ce} + \text{Y})$ diagram (after Eby, 1990). FG-field for fractionated I-type granitoids; OGT-field for I-, S- and M-type granitoids.

Data source of the Daolinshan granites and Shangshu rhyolites is from Li et al. (2008b) and Wang et al. (2010b).

effect during the weathering of arc-derived materials (Zheng et al., 2008).

6.3. Minjiawu volcanics

The Minjiawu volcanics have SiO_2 contents ranging from 52.1 to 64.6 wt%. TiO_2 contents are below 1.0 wt% (0.29–0.90 wt%). Except for sample 10JX-3-1 which has the highest MgO content (8.07 wt%) and $\text{Mg}^{\#}$ (62), the volcanics have high Al_2O_3 contents (17.6–19.1 wt%) and low $\text{Mg}^{\#}$ (from 29 to 49). The Minjiawu volcanics (except for sample 09JX-7-1) have high $\text{Na}_2\text{O}/\text{K}_2\text{O}$ ratios (from 5.92 to 47.58). Sr/Y ratios are higher for these Na-rich rocks, ranging from 22 to 242. The Y contents (from 10.7 to 18.3 ppm) and Yb contents (from 0.94 to 2.0 ppm) of the Na-rich rocks are basically lower than 18 and 1.9 ppm, respectively, which resemble those of typical adakitic rocks (Defant and Drummond, 1990).

The intermediate rocks have relatively high REE contents and steep LREE patterns (Fig. 11a), with $(\text{La}/\text{Yb})_N$ values of 5.54–5.64. They have scattered and high LILE contents, strongly positive Pb

anomalies and evident Zr and Hf positive anomalies (Fig. 11b), similar to the Xucun granitic porphyries. The mafic rocks have relatively low REE contents, and weak positive Eu anomalies (Fig. 11a; Table 2). The positive anomalies in Ba, Pb, and Sr are evident in these samples (Fig. 11b). The contents of other LILEs and incompatible elements are very low. Especially the Th, U, K, Nb and Ta contents are lower than those of typical oceanic-arc basalts (OCB). The negative anomalies in Nb and Ta are evident, and there are no positive anomalies of Zr and Hf (Fig. 11b), suggesting that the magma source may be related to the subduction of the oceanic slab.

The Minjiawu volcanics show initial $^{87}\text{Sr}/^{86}\text{Sr}$ ratios ranging from 0.7040 to 0.7047. The $^{143}\text{Nd}/^{144}\text{Nd}$ ratios are high (from 0.512476 to 0.512613), generating positive $\varepsilon_{\text{Nd}}(t)$ values of +3.7 to +4.8 (Table 3), suggestive of a depleted-mantle source.

6.4. Shangshu bimodal volcanics

The mafic rocks of the Shangshu bimodal volcanics can be divided into two subgroups. Group 1 has relatively high $\text{Mg}^{\#}$ (from

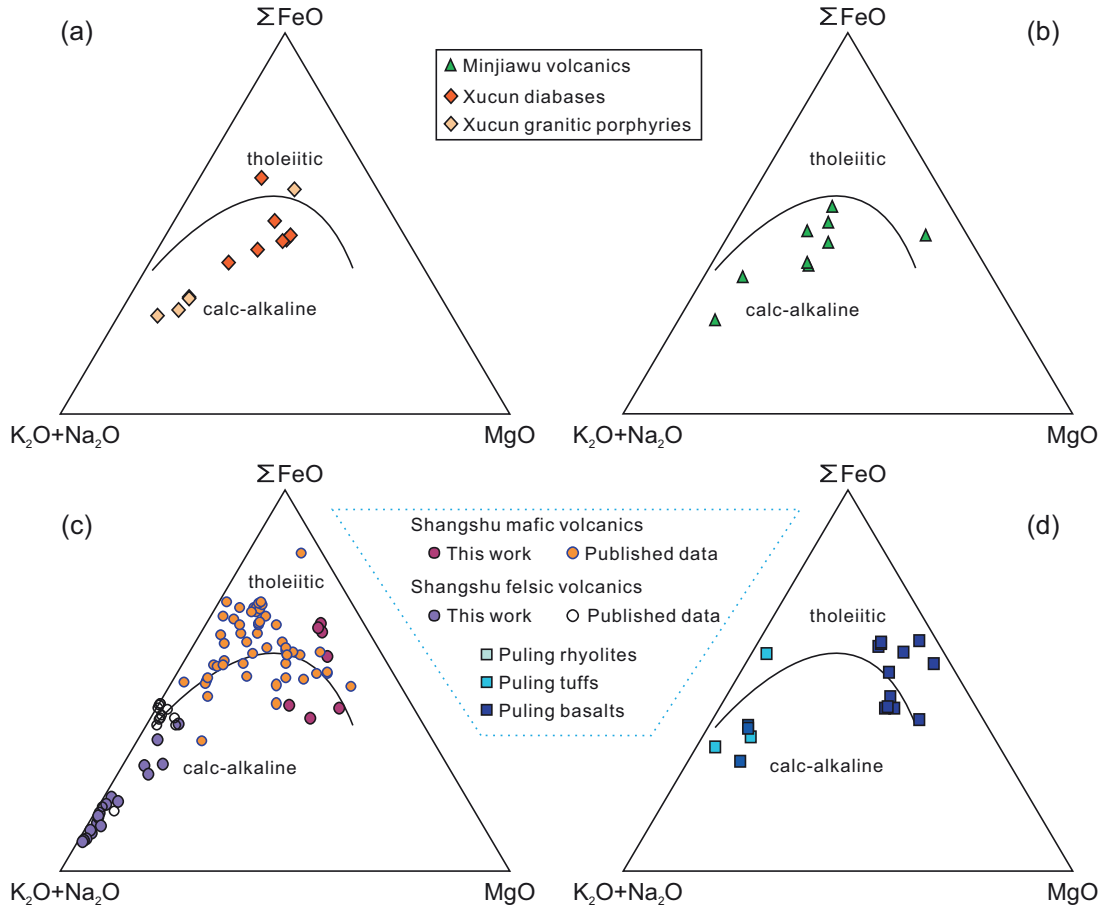


Fig. 9. AFM diagrams showing the volcanic rocks in the eastern part of the Jiangnan orogen (after Irvine and Baragar, 1971). (a) the Xucun composite dykes; (b) the Minjiawu volcanics; (c) the Shangshu bimodal volcanics; (d) The Puling bimodal volcanics. Data for the Shangshu bimodal volcanics are from Li et al. (2008b).

54 to 62) and enriched LREE ($(\text{La/Yb})_N$ of 8.77–13.7) (Fig. 11c; Table 2). Fractionations of MREE relative to HREE are also evident, with $(\text{Gd/Yb})_N$ values varying from 2.3 to 2.8. The negative anomalies in Nb, Ta, Zr and Hf are evident in these samples (Fig. 11d). The trace-element distribution patterns are basically similar to those of typical continental-arc basalts, but rather different from those of oceanic-island basalts (OIB) (Fig. 11d). Group 2 has relatively low $\text{Mg}^{\#}$ (41–49). Fractionations of LREE relative to HREE are not evident in these samples (Fig. 11e), with $(\text{La/Yb})_N$ values of 2.2–3.7. One sample (10SS-10-3) has negative Ce anomaly, as well as positive anomalies of Rb, Ba and K (Fig. 11f), which may reflect the observed alteration. The LILE contents are clearly lower than those of OIB. The negative anomalies in Nb and Ta are also evident, similar to those of average continental-arc basalts. However, the positive anomalies in Zr and Hf, as well as the high TiO_2 contents (1.54–3.13 wt%) resemble those of OIB.

The Shangshu rhyolites generally have high SiO_2 contents, with most samples ranging from 69.8 to 76.8 wt% (Table 2). K_2O contents are mostly higher than Na_2O . These rocks have clearly negative anomalies in Eu, Nb, Ta, Sr, P, and Ti (Fig. 11g and h), similar to many Neoproterozoic granitoids along the Jiangnan orogen (Li et al., 2003a, 2008b).

Most of the Shangshu bimodal volcanics have high Rb/Sr ratios, leading to unreasonably high initial $^{87}\text{Sr}/^{86}\text{Sr}$ ratios (Table 3). Samples 10SS-3-4 and 10SS-10-2 have initial $^{87}\text{Sr}/^{86}\text{Sr}$ ratios of 0.7089 and 0.7110, respectively, possibly suggesting the incorporation of crustal materials in their magma source, or crustal contamination

during eruption. Sample 10SS-3-4 has the highest $\varepsilon_{\text{Nd}}(t)$ (+6.2), suggesting a depleted-mantle source. The mafic rocks of Group 2 have relatively low $\varepsilon_{\text{Nd}}(t)$ values, ranging from +1.4 to +2.7 (Table 3). The $\varepsilon_{\text{Nd}}(t)$ values of the rhyolites range from -1.9 to +0.4.

6.5. Puling formation

The basalts from the Puling Formation have similar geochemical features, except for sample 09JX-2-7 which has high TiO_2 (2.4 wt%) and low Zr/Nb ratio (16.8). The other basalts have TiO_2 contents ranging from 0.56 to 0.87 wt%, and $\text{Mg}^{\#}$ from 44 to 67. The enrichment of LREE (except La) is not evident (Fig. 12a). One sample (09WN-3-2) has fractionated HREE, probably suggesting the presence of residual garnet in the source. The nearly flat distributions of REE are similar to those of typical arc volcanics in subduction settings. The negative anomalies in Nb and Ta are evident (Fig. 12b). Most of the samples have low abundances of LILE HFSE. Overall, the trace-element distribution patterns of these basalts are similar to those of the average arc basalts, and completely different from those of OIB (Fig. 12b). However, sample 09JX-2-7 has enriched LREE (Fig. 12a) and HFSE (Fig. 12b), without negative anomalies in Nb and Ta, and is rather similar to that of the Group 2 mafic rocks of the Shangshu bimodal volcanics. This sample has the highest $\varepsilon_{\text{Nd}}(t)$ (+6.2), and the other basalts have $\varepsilon_{\text{Nd}}(t)$ ranging from +1.3 to +3.1.

The tuffs and rhyolites of the Puling formation have geochemical features similar to the Shangshu rhyolites. Negative Eu anomalies are evident (Fig. 12c). However, negative Ba anomalies are absent

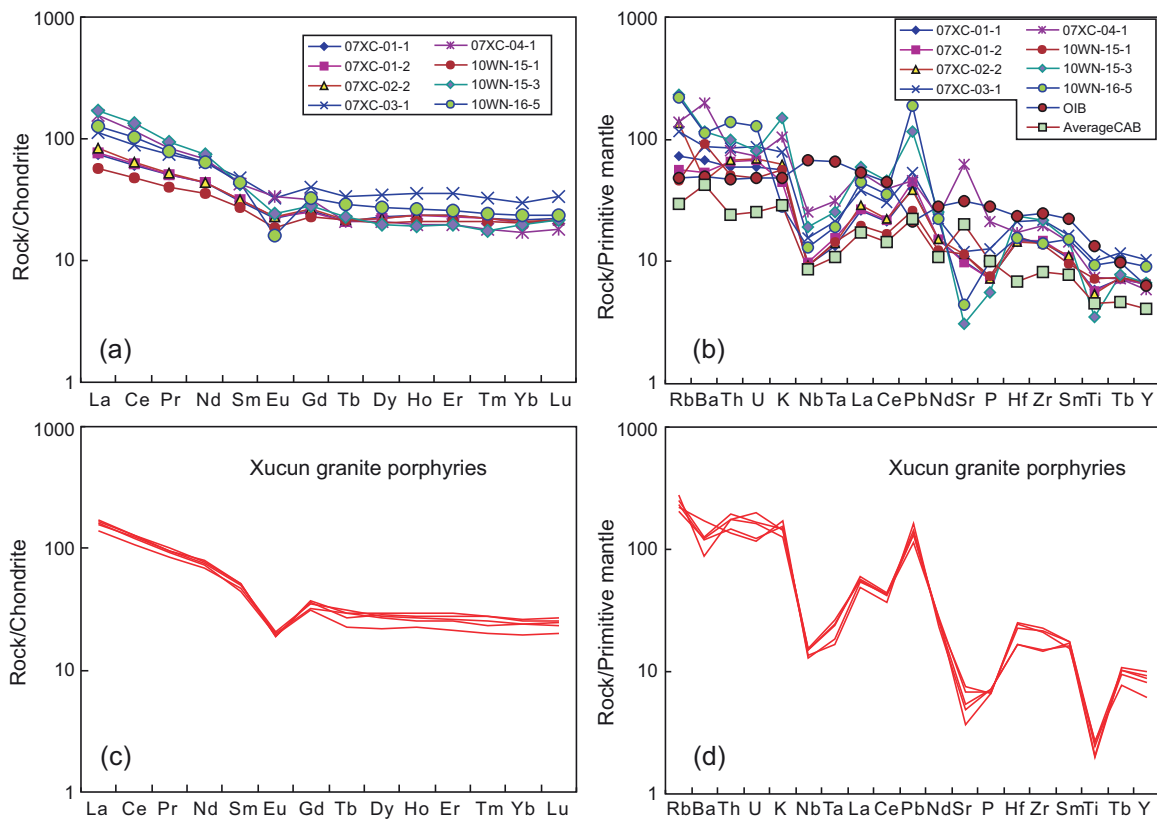


Fig. 10. Normalized REE and trace-element patterns for the rocks of the Xucun composite dykes. Chondrite, primitive-mantle and ocean island basalt (OIB) data are from Sun and McDonough (1989).

The data for average continental arc basalts (CAB) are from Kelemen and Hanghøj (2004).

in these rocks (Fig. 12d). Their Nd isotopes suggest LREE enrichment and low Sm/Nd, with $\varepsilon_{\text{Nd}}(t)$ of -9.8 , giving in Paleoproterozoic model ages of 2230–2233 Ma.

7. Discussion

7.1. Magmatic processes and crustal contamination

In contrast to the ca 850–820 Ma magmatism in the eastern part of the Jiangnan orogen, which is dominated by intrusive rocks (Wang et al., 2006), the ca 800–760 Ma magmatic rocks in the area are dominated by volcanic rocks with compositions ranging from basaltic to granitic. Therefore, it is necessary to discuss the genetic relationship between the different rock types and to evaluate the role of crustal contamination in their petrogenesis. The crustal contamination can be monitored by plots involving the Nd isotopes. Rough negative correlations between SiO₂ and $\varepsilon_{\text{Nd}}(t)$ can be observed in the Xucun and Puling mafic rocks (Fig. 13a), implying the crustal contamination. The weak positive correlation in the Shangshu mafic rocks probably is not significant because two samples with clearly low SiO₂ contents may have undergone significant alteration. The Minjiawu volcanics have constant $\varepsilon_{\text{Nd}}(t)$ (Fig. 13a), precluding significant crustal contamination. The 1/Nd vs $\varepsilon_{\text{Nd}}(t)$ diagram (Fig. 13b) shows similar results. Meanwhile, the two diagrams involving the Nd isotopes also reveal clear differences between the mafic and felsic rocks, suggesting that the felsic rocks are not the products of fractional crystallization of mafic magmas.

7.2. Partial melting of juvenile crustal materials

As discussed above, felsic rocks dominated the Neoproterozoic magmatic activity during ca 800–760 Ma. Studies of the felsic rocks

can shed light on the crustal evolution in the area. The Shangshu rhyolites are strongly peraluminous in composition, and do not resemble the A-type granites (Fig. 8d), suggesting that they may have been derived dominantly from the partial melting of meta-sedimentary sources; this is consistent with the published $\delta^{18}\text{O}$ values of zircons (6.52–8.98) (Zheng et al., 2008). Their $\varepsilon_{\text{Nd}}(t)$ values range from -1.9 to $+0.4$, indicating the incorporation of some juvenile crustal materials in their magma source. Similarly, the ca 820 Ma granitoids in the eastern part of the Jiangnan orogen have whole-rock $\varepsilon_{\text{Nd}}(t)$ from -0.20 to -3.11 (Li et al., 2003b) and contain zircons with the late Mesoproterozoic to early Neoproterozoic Hf model ages, generating a peak at ca 1.15 Ga. The Xucun granitic porphyries have similar zircon Hf isotopes, with a mean $\varepsilon_{\text{Hf}}(t)$ of $+3.8 \pm 0.7$ and an average T_{DM1} of 1222 ± 26 Ma.

The Hf isotopes of zircons may be more reliable in tracing the sources of the felsic rocks. Zheng et al. (2008) interpreted the late Mesoproterozoic (Grenvillian?) Hf model ages as defining a major episode in the growth of juvenile crust related to the arc magmatism in the Jiangnan orogen. However, there is no definite record of magmatism in the Jiangnan orogen during this period. The volcanic rocks in the Shuangxiwu area of northwest Zhejiang Province have been widely accepted as representing arc magmatism in the eastern part of the Jiangnan orogen, and the available zircon U-Pb ages suggest an approximate duration of ca 930–880 Ma for this magmatism (Cheng, 1991; Zhou and Zhu, 1993; Wang et al., 2007; Li et al., 2009). These rocks have very high $^{176}\text{Hf}/^{177}\text{Hf}$ (Chen et al., 2009; Li et al., 2009), representing the growth of juvenile crust under the subduction regime in the area. At present, there is not enough evidence for the partial melting of late Mesoproterozoic juvenile crustal materials. Hence, it may be more reasonable to interpret the Neoproterozoic (ca 820–760 Ma) felsic magmatic rocks as products of partial melting of early Neoprotero-

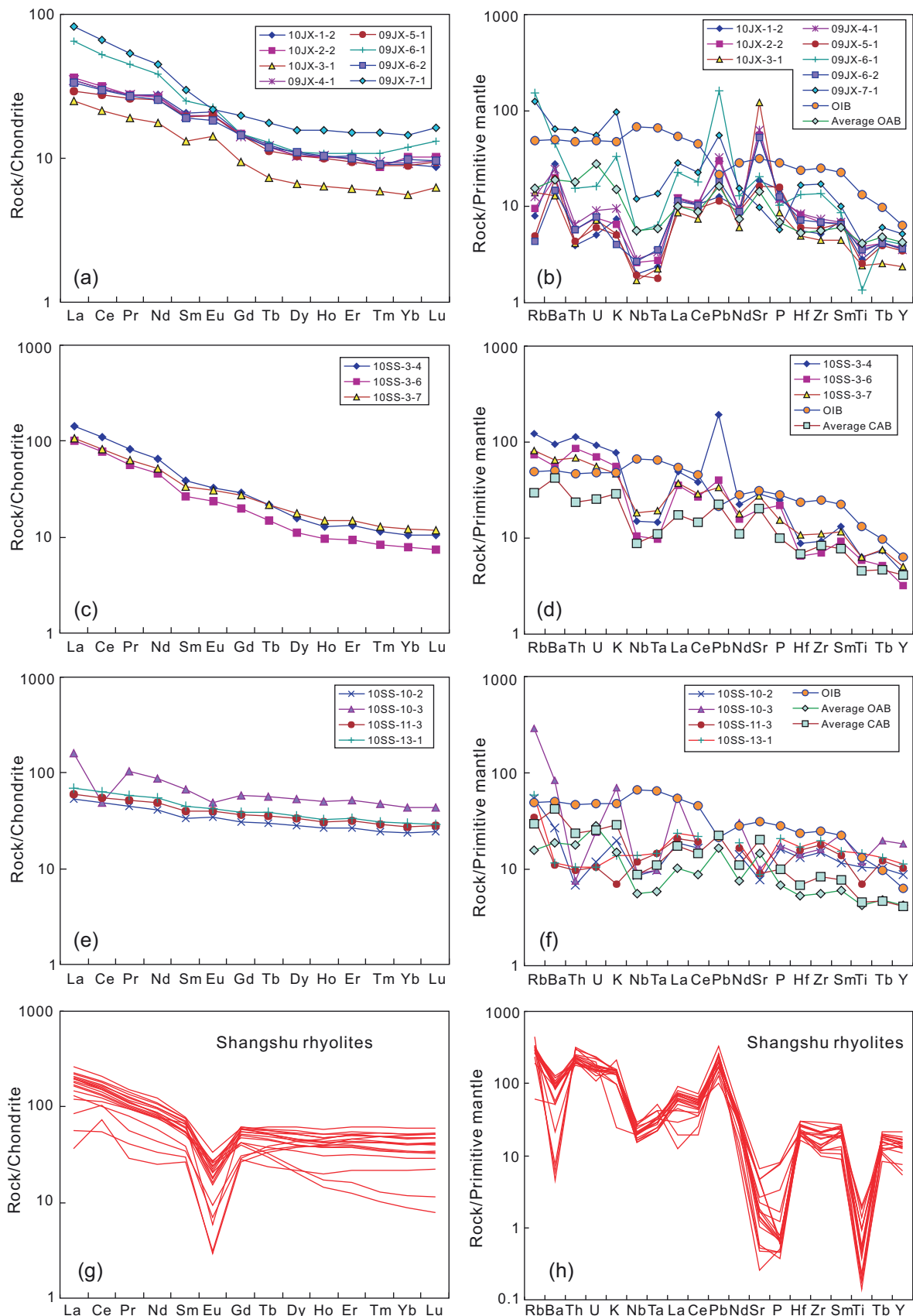


Fig. 11. Normalized REE and trace-element patterns for the volcanic rocks of the Shangshu Formation. Chondrite, primitive-mantle and ocean island basalt (OIB) data are from Sun and McDonough (1989).

The data for average oceanic and continental arc basalts (CAB) are from Kelemen and Høegh (2004).

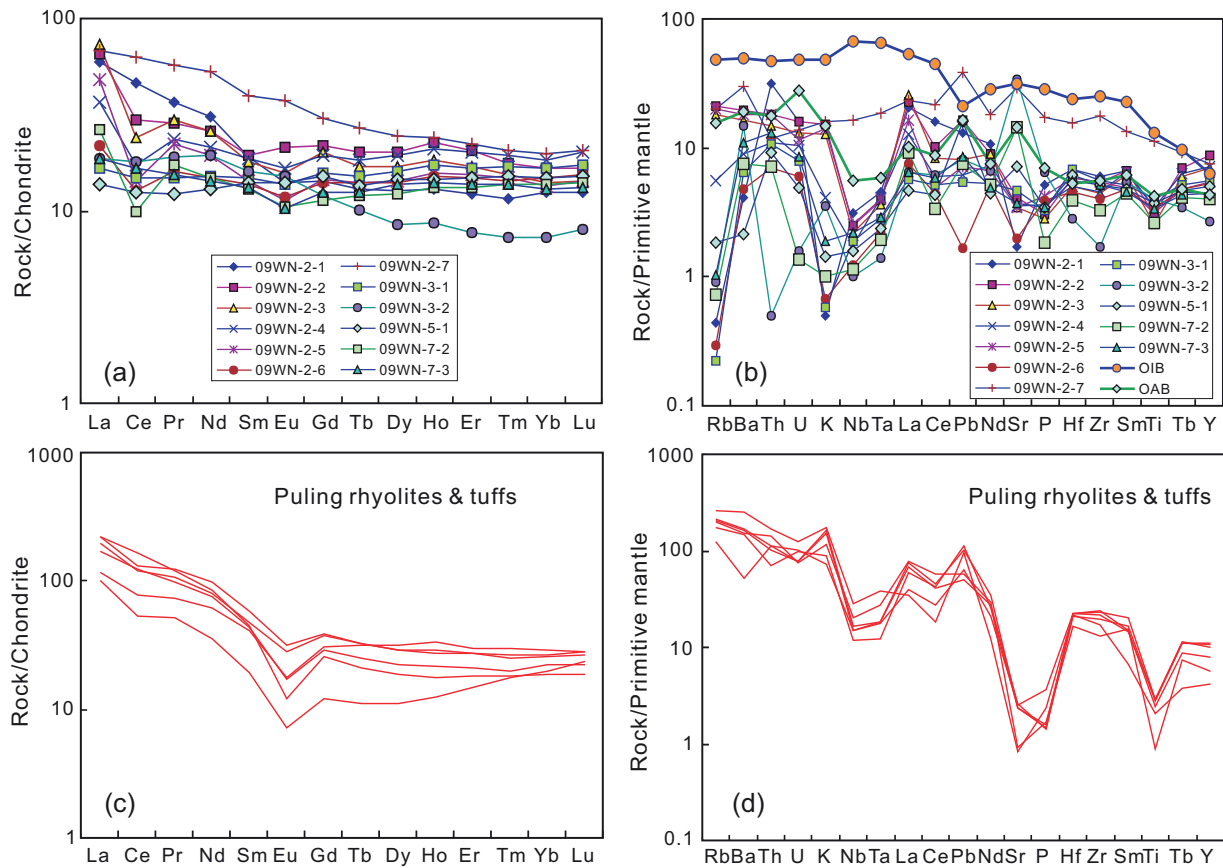


Fig. 12. Normalized REE and trace-element patterns for the Puling bimodal volcanic rocks. Chondrite, primitive-mantle and ocean island basalt (OIB) data are from Sun and McDonough (1989).

The data for average oceanic-arc basalts (OAB) are from Kelemen and Hanghøj (2004).

zoic juvenile crustal materials. The weathering and later reworking of arc-derived rocks in the late or post-orogenic stages would then explain the high $\delta^{18}\text{O}$ and $\varepsilon_{\text{Nd}}(t)$.

One exceptional spot analysis of zircon from the Xucun granitic porphyries has negative $\varepsilon_{\text{Hf}}(t)$ value (-4.11 ± 0.90) and a calculated Hf T_{DM2} of 1971 ± 36 Ma. This age is clearly older than the whole-rock Nd T_{DM2} (from 1417 to 1506 Ma), indicating that the incorporation of Paleoproterozoic crustal components may not be

negligible. To the west of the Xucun composite dykes, the role of Paleoproterozoic crust is more evident as the Puling tuffs and rhyolites give whole-rock Nd T_{DM2} ranging from 2230 to 2233 Ma. The westward increase in the role of Paleoproterozoic crustal materials suggests the strengthening of the Yangtze basement. Therefore, the NE-Jiangxi Fault may be the boundary between the Neoproterozoic accretionary arc terrane and the Yangtze continental block.

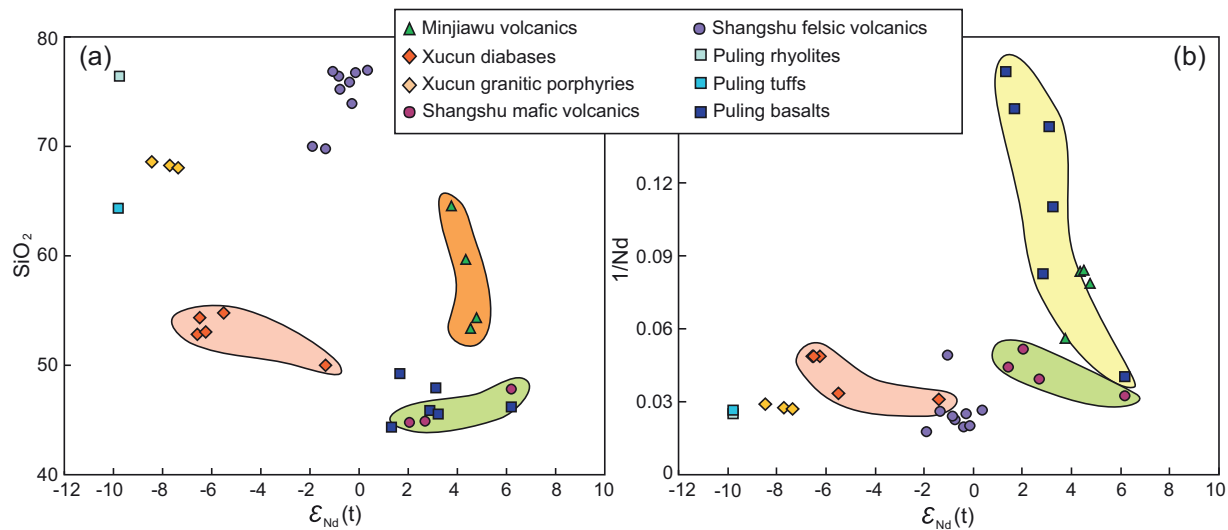


Fig. 13. Crustal-contamination discrimination diagrams for the volcanic rocks in the eastern part of the Jiangnan orogen.

7.3. Diversity of magma sources for the mantle-derived rocks

The widespread partial melting of different crustal components in the SCB requires subcrustal heating, while the mantle-derived rocks may record useful clues for the mantle dynamics and geological processes. The different types of trace-element distribution patterns suggest considerable complexity in the magma sources of the mantle-derived rocks in the eastern part of the Jiangnan orogen.

7.3.1. Xucun diabase dykes

The diabases from the Xucun composite dykes have trace-element patterns similar to those of OIB, except for the depletions in Nb, Ta, Sr and P. Sample 07XC-4-1 has the lowest SiO₂ content (50.0 wt%) and weakest depletions in Nb and Ta (Fig. 10b), as well as an un conspicuous positive Pb anomaly. Moreover, it has the highest $\varepsilon_{\text{Nd}}(t)$ (-1.38) among the Xucun composite dykes, obviously different from other samples whose $\varepsilon_{\text{Nd}}(t)$ falls into the range of -5.50 to -6.57. These differences suggest that this sample experienced the lowest degree of crustal contamination and thus could be used as a proxy for the primary composition of the magma. A positive Sr anomaly is evident in the sample, precluding significant fractional crystallization of plagioclase, which is consistent with the absence of a negative Eu anomaly. The high abundances of incompatible elements in the Xucun diabases imply that they are not continental-arc basalts. It should be noted that one Hf spot analysis from zircons of the diabase has a very depleted $\varepsilon_{\text{Hf}}(t)$ of +14.5, indicating the existence of extremely depleted mantle components in the magma source. Therefore, it can be deduced that the composition of the primary magma of the diabases would have higher 143Nd/144Nd and weaker depletions in Nb and Ta than sample 07XC-4-1, which has the most radiogenic Nd isotopes.

The other diabases have similar $\varepsilon_{\text{Nd}}(t)$ values and trace-element patterns similar to those of the granitic porphyries in the composite dykes (Fig. 10), indicating crustal contamination or element exchange. However, the major elements are different between the rocks, suggesting the trace-elements patterns and isotopic compositions may be more easily affected by contamination or metasomatism than the major elements (Lesher, 1990). One sample from the mafic dykes is intermediate in composition (SiO₂ = 61.52 wt%), probably representing local magma mixing.

7.3.2. Minjiawu volcanic rocks

The Minjiawu mafic rocks have low LILE and HFSE contents and evident depletions in Nb and Ta. These are clearly the geochemical features of basalts generated in subduction regimes. The depletions in Th, U and K may be inherited from the magma source. Their $\varepsilon_{\text{Nd}}(t)$ values range from +4.3 to +4.8, indicating a LREE-depleted magma source and negligible crustal contamination. The negative anomalies in Zr and Hf are generally explained as the result of partial melting in subduction settings (Zhou et al., 2006b). Li et al. (2007) suggested the fractional crystallization of pyroxenes as an alternative explanation. However, the fractional crystallization of pyroxenes will elevate the abundances of incompatible elements, which is not consistent with the trace-element patterns of the mafic rocks. Sample 10JX-3-1 has the highest MgO content (8.1 wt%) and Mg[#] (62), suggesting that it may have been generated from a primitive magma, and thus could reflect the geochemical feature of the magma source. The sample has extremely weak Nb depletion and low abundances of REE and most HFSE. The Na₂O/K₂O ratio is high (10), although the Na₂O content is a bit lower than in the other mafic samples. The Na-enrichment in the magma source suggests the partial melting of subducted oceanic slab (Zhou et al., 2006b). However, the Minjiawu mafic rocks may not be derived directly from the subducted oceanic slab, because the fractionations between LREE, MREE and HREE are not significant (Fig. 11a), in contrast to typical adakites as defined by Defant and Drummond (1990). Therefore,

the partial melting of lithospheric mantle metasomatized by Na-rich melts from the subducted oceanic slab may be a reasonable explanation for the genesis of the mafic rocks in the Minjiawu area.

The intermediate rocks have initial Sr isotopic ratios similar to those of the mafic rocks, indicating a similar magma source. The relatively low $\varepsilon_{\text{Nd}}(t)$ (+3.7) suggests that they might have experienced crustal contamination and/or AFC processes during the ascent of the mafic magma. The weak depletions of MREE in the intermediate rocks indicate that hornblende may exist as a residual phase in the magma source.

7.3.3. Shangshu and Puling mafic rocks

Two types of magma source are identified for the mafic rocks from the Shangshu and Puling bimodal rock suites.

Group 1 samples of the Shangshu mafic rocks are depleted in Nb, Ta, Zr and Hf, resembling average continental-arc magmatism. They have relatively low TiO₂ contents and Zr/Sr and Nb/La ratios, and high Mg[#] (54–62), suggesting the partial melting of metasomatized lithospheric mantle, similar to the ca 820 Ma mafic-ultramafic rocks in northern Guangxi (Wang et al., 2006). One sample has a high $\varepsilon_{\text{Nd}}(t)$ of +6.2, indicating that the metasomatism probably was not much older than the eruption of the mafic rocks. Group 2 samples of the Shangshu mafic rocks have no depletions in Zr and Hf or no negative anomalies in Nb and Ta (samples 10SS-11-3 and 10SS-13-1), and may not have resulted from the partial melting of metasomatized lithospheric mantle. Their relatively high contents of TiO₂ and Zr (169–221 ppm) and Zr/Sr ratios (32.3–32.6, except for sample 10SS-10-3) resemble the basalts formed in within-plate settings, suggesting that they may have been generated from the partial melting of asthenospheric mantle. The relatively low $\varepsilon_{\text{Nd}}(t)$ values (+1.4 to +2.7) may result from crustal contamination or mixing with metasomatized lithospheric mantle.

Sample 09WN-2-7 is an exceptional among the Puling mafic rocks. It has a high TiO₂ content (2.41 wt%), and high Nb/La (0.73) and Zr/Sr (32.9) ratios, without depletions in Nb, Ta, Zr and Hf, similar to the Group 2 mafic rocks in the Shangshu bimodal volcanics. Its high $\varepsilon_{\text{Nd}}(t)$ (+6.18) is consistent with a depleted asthenosphere source. The weak Pb positive anomaly implies little crustal contamination. The other mafic rocks from the Puling bimodal volcanics show evident depletions in Nb and Ta and overall OCB-like geochemical patterns, indicating that they may have been generated from the partial melting of metasomatized lithospheric mantle. They have low abundances of LREE, and some of them exhibit flat REE patterns, suggesting a high degree of partial melting.

7.4. Tectonic settings: arc, plume or post-orogenic?

Due to the possible relationship with the assembly and rifting of the Rodinia supercontinent, the Neoproterozoic (ca 850–750 Ma) magmatic rocks in the Jiangnan orogen have received great attention in recent years (e.g., Li et al., 2003a,b, 2008a,b; Zhou et al., 2004, 2009; Wang et al., 2004, 2006, 2008a, 2010b). Two age peaks are identified for the magmatism in the SCB: ca 820 Ma and ca 780 Ma. Igneous rocks erupted in these two time intervals along the Jiangnan orogen have been considered as the results of post-collisional and post-orogenic extension, respectively (Wang et al., 2006, 2008a). The mid-Neoproterozoic magmatism in the eastern part of the Jiangnan orogen is more complex than that in the western part and its tectonic settings remain uncertain. The Shangshu volcanic rocks have been suggested to be generated in an arc setting (Shu et al., 1995), mainly based on their arc-like geochemical features. However, it is invalid to distinguish tectonic settings based simply on the geochemical features, since the geochemistry of single rock series is only an indicator of their magma source and crystallization processes. As discussed above, the volcanics of the Shangshu Formation, as well as the Xucun composite dykes

and Puling Formation, show a bimodal distribution of composition, usually found in extensional environments. Some rocks have the geochemical features of within-plate basalts and may result from the partial melting of asthenospheric mantle, supporting this conclusion. Therefore, a simple arc model may not be appropriate in explaining the formation of the *ca* 800–760 Ma volcanic rocks.

The “plume” model first proposed by Li et al. (1999) was adopted by some scholars to explain the mid-Neoproterozoic magmatic rocks in the SCB (e.g., Li et al., 2003a, 2003b, 2008b). However, this model may not be appropriate in the eastern part of the Jiangnan orogen, based on two lines of geological evidence.

- (1) There are no significant plume-related magmatic rocks (including CFB, alkaline basalts, high-Mg basalts, etc.) in the Jiangnan orogen. The *ca* 760 Ma OIB-like mafic rocks reported in the western part of the Jiangnan orogen (Wang et al., 2008a) are only alkaline in geochemical composition, rather than in mineralogy, and they have an outcrop area less than 10 km². The *ca* 820 Ma komatiitic basalts in central Jiangnan orogen have high MgO contents and Mg# values (Wang et al., 2004), and were considered to be related to the Neoproterozoic plume activity (Wang et al., 2007b). However, the partial melting of sub-arc refractory mantle after extraction of typical arc melts is a more reasonable explanation (Zheng et al., 2008). The absence of significant plume-related rocks at the initiation of the magmatism (*ca* 820 Ma) and the following main rifting period (*ca* 780 Ma) preclude the “plume” model.
- (2) The amount of magmatic rocks is not necessarily related with plume activities. A Large Igneous Province (LIP) is a good indicator of plume activity within the continental plates (e.g., Ernst et al., 2005), and generally covers an area of at least 50,000 km² (Sheth, 2007), and the rocks have geochemical features similar to CFB. However, the mid-Neoproterozoic magmatic rocks in the eastern part of the Jiangnan orogen only cover an area of *ca* 6000 km² (based on geological reports), among of which *ca* 5000 km² are felsic rocks (including granitoids, rhyolites and etc.). These characteristics of mid-Neoproterozoic magmatic rocks in the eastern part of the Jiangnan orogen therefore do not fit the definition of a LIP.

Wang et al. (2008a) proposed a post-orogenic extension model for petrogenesis of the *ca* 770–750 Ma magmatic rocks in the western part of the Jiangnan orogen. As discussed above, the volcanic rocks in the eastern part of the Jiangnan orogen were generated in extensional settings, which can be easily accomplished in the post-orogenic stage. During the orogenic processes, slab-breakoff is a natural process following the assembly of two blocks or terranes (Davies and Blanckenburg, 1995). This is still within the orogenic regime although extension has started (Bonin, 2004). Due to the thickening of crust and the delamination resulting from melt extraction in the orogenic and post-collisional stages, the collapse of the orogen takes place (e.g., Dewey, 1988; Draut et al., 2002). The strong upwelling of the asthenospheric mantle and the accompanying intense extension may lead to the partial melting of previously-metasomatized lithospheric mantle and the overlying crust. In addition, the ascending asthenospheric mantle may be melted when it reaches a certain level.

The diverse magma sources for the *ca* 800–760 Ma mafic volcanic rocks in the eastern part of the Jiangnan orogen may have developed during the post-orogenic stage. In other words, these rocks could be generated in a normal evolutional process of an orogenic belt. The absence of significant alkaline rocks or large amounts of basaltic rocks suggests that the rifting represented by the *ca* 800–760 Ma volcanic rocks was passive, rather than active,

and was related to the natural evolution of the Jiangnan orogen. The signatures of metasomatized lithospheric mantle revealed by the volcanics of the Shangshu and Puling Formations may be inherited from the subduction processes during the early Neoproterozoic assembly of the Yangtze and Cathaysia blocks. The features of an asthenosphere source revealed by the Xucun mafic rocks and some volcanic rocks from the Shangshu and Puling Formations may imply the partial melting of the upwelling asthenospheric mantle during the post-orogenic extension stage. This post-orogenic stage represents in fact the anorogenic setting that immediately followed the orogenic processes, representing the ending of a Wilson cycle, different from the post-collision extension that belongs to the orogenic cycle. According to the definitions of Bonin et al. (1998), the post-orogenic stage is characterized by bimodal alkaline rock suites. The available published data show that the *ca* 800–790 Ma Shangshu rhyolites (Li et al., 2008b) and *ca* 790–780 Ma Daolinshan granites (Li et al., 2008b; Wang et al., 2010b) are geochemically similar to A2-type granites, although the rocks of this study do not show this feature. However, alkaline mafic rocks have not been found in the eastern part of the Jiangnan orogen, probably suggesting that the extension in the area was not intense enough. High ¹⁴³Nd/¹⁴⁴Nd has been considered as another feature of post-orogenic magmatism (Bonin, 2004). Some primitive samples from this study have high ε_{Nd}(t) values, consistent with the upwelling of deep asthenospheric mantle, and supporting the post-orogenic model.

7.5. Post-orogenic extension along the Jiangnan orogen: Part of the Rodinia rifting?

The mid-Neoproterozoic magmatism related to the post-orogenic extension may have occurred along the whole Jiangnan orogen. The post-orogenic mafic rocks in the western part of the Jiangnan orogen occur within the Banxi Group and the Danzhou Group, which can be compared with the Shangshu Formation (Wang and Li, 2003). However, the post-orogenic extension may have been diachronous. The extension may have taken place earlier in the eastern part of the Jiangnan orogen, leading to the formation of the *ca* 800 Ma Xucun composite dykes and the continental volcanic rocks of the Shangshu Formation. However, the Banxi Group and Danzhou Group in the western part of the Jiangnan orogen are marine sequences (Wang and Li, 2003), without significant continental magmatism. This probably suggests that the marine basin in the western part of the Jiangnan orogen did not close when the orogenic processes ended in the eastern part of the orogenic belt. The tectonic setting of the western part of the Jiangnan orogen may change from post-collisional extension to post-orogenic extension when the deposition of Hetong Formation of the Danzhou Group took place. A great amount of sub-alkaline mafic-ultramafic intrusive rocks and pillow spilites erupted at *ca* 770 Ma in the Hetong Formation in northern Guangxi Province, whereas the post-orogenic extension tended to be weaker in the eastern part of the Jiangnan orogen. At *ca* 760 Ma, the Puling bimodal volcanics erupted, revealing the continuing dominant partial melting of metasomatized lithospheric mantle. However, the mafic rocks in western Hunan Province imply the partial melting of asthenospheric mantle as suggested by Wang et al. (2008a). Similar diachronous post-orogenic extension is reported in South America in Paleoproterozoic time (Teixeira et al., 2002). The diachronous extension implies that the formation of mid-Neoproterozoic (*ca* 800–750 Ma) magmatic rocks in the Jiangnan orogen may have no direct relationship with the subduction along the western and northwestern margins (Zhou et al., 2006b; Zhao et al., 2011) of the Yangtze Block.

The post-orogenic extension represented by the *ca* 800–760 Ma magmatic rocks is a natural consequence of the orogenic cycle

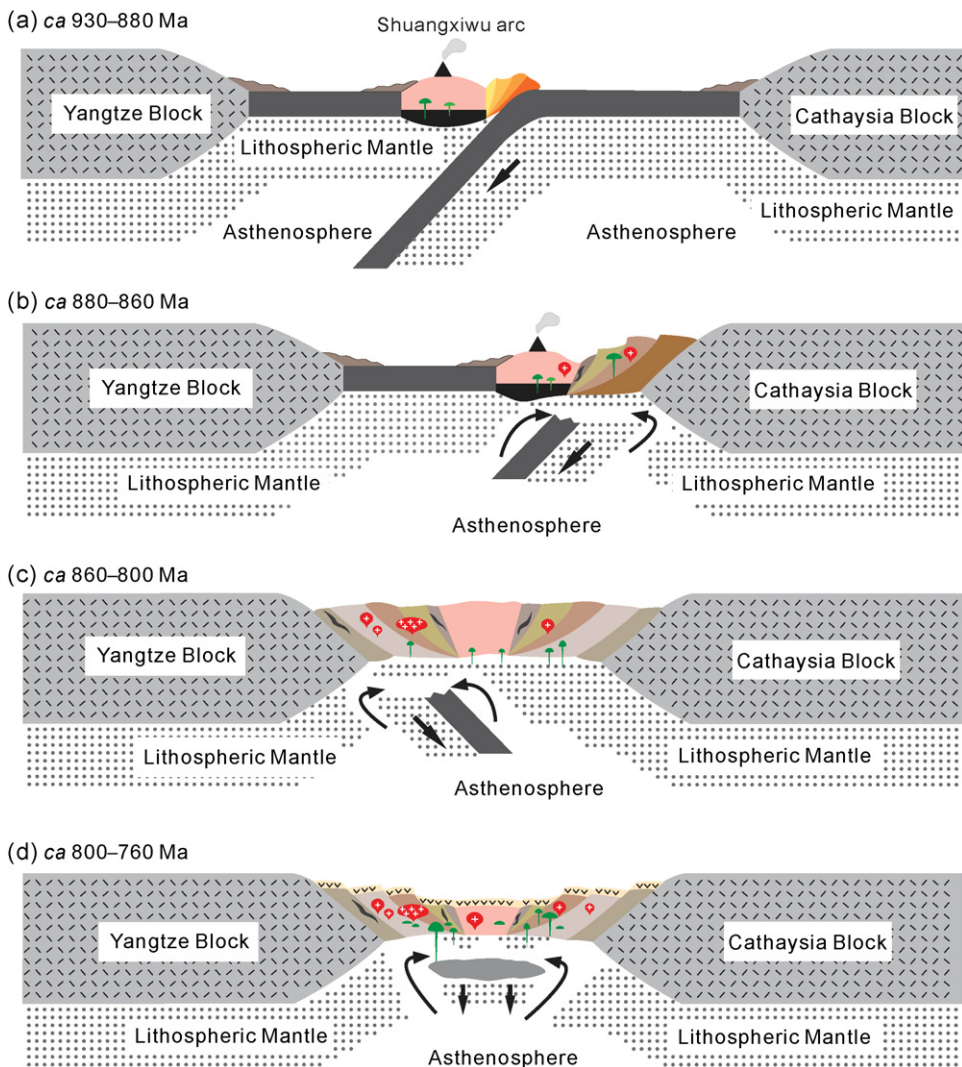


Fig. 14. Simplified cartoon model for the evolution of the eastern part of the Jiangnan orogen from *ca* 930–760 Ma. Ocean–ocean subduction led to the formation of island arc volcanic in the Shuangxiwu area at *ca* 930–880 Ma; (b) Arc–continent collision took place at *ca* 880–860 Ma, which led to the syn-collisional deformation and magmatism in the arc–continental collisional belt. (c) Following the closing of the back-arc basin, the basement sequences were folded; then the extension in the post-collisional regime and the accompanying upwelling of deep asthenosphere led to the partial melting of the crustal materials that may have been mainly derived from the erosion of the arc terrane, forming widespread granitoids along the Jiangnan orogen. (d) The continuing partial melting of the mid- to lower crust led to the residual lower crust becoming denser. The Jiangnan orogen entered into the post-orogenic stage at *ca* 800–760 Ma. Bimodal volcanic activity developed during the period. The partial melting of metasomatized lithospheric mantle and upwelling asthenosphere took place together.

of the Jiangnan orogen. As proposed by [Wang and Li \(2003\)](#), the volcano-sedimentary sequences represent a rifting environment in the area. The rifting resulting from the post-orogenic extension in the Jiangnan orogen is roughly contemporaneous with the rifting of the Rodinia supercontinent. Similarly, *ca* 780 Ma extension-related magmatism has been reported along the western and northwestern margins of the SCB ([Huang et al., 2008](#); [Hu et al., 2010](#)). From this point of view, the *ca* 800–760 Ma widespread extension of South China may be part of the global Neoproterozoic rifting events that finally led to the breakup of the supercontinent, although the failed rift in South China did not move the Yangtze Block away from Cathaysia ([Li et al., 1995](#)). The Neoproterozoic rift was significantly overprinted by the later Caledonian movement ([Charvet et al., 1996](#)). Since the post-orogenic magmatic activity was not particularly intense, it may not have been the engine for the breakup of the Rodinia supercontinent. If Rodinia was split due to a super-plume as suggested by [Li et al. \(2003b\)](#), the SCB may not have been located in the interior of the supercontinent where the rifting would be most intense.

7.6. Tectonic model

The above detailed studies on magma sources and tectonic settings of the *ca* 800–760 Ma volcanic rocks may shed light on the evolution of the Jiangnan orogen. The extremely depleted Nd–Hf isotopic features of the volcanic rocks in the Shuangxiwu Group of northern Zhejiang Province, as well as the large amounts of the late-Mesoproterozoic to early Neoproterozoic Hf model ages of zircons from the Neoproterozoic igneous rocks, indicate that there was an oceanic subduction in the early Neoproterozoic, which finally led to the formation of the Shuangxiwu island arc at *ca* 930–880 Ma ([Fig. 14a](#)). This NW-dipping subduction (present coordinates) is supported by the distributions of foreland basin, back-arc basin, syn-collisional magmatic rocks in the area and the kinematic studies ([Charvet et al., 1996](#); [Shu and Charvet, 1996](#)). At *ca* 880–860 Ma, arc–continent collision took place, and some syn-collisional magmatic rocks were intruded at this period ([Fig. 14b](#)). Following slab-breakoff and delamination of the lower crust of the arc–continent collisional belt, a new subduction event may be initiated in the back-arc area, which led to the metasomatism of the

newly-formed lithospheric mantle beneath the western part of the arc terrane. The volcanic rocks formed at this period may now be mostly eroded due to the following uplift of the orogen, and provided abundant material for the strata in the back-arc basin, i.e. the Shuangqiaoshan Group, as we can see from the detrital zircons in the sediments (Wang et al., 2007). The back-arc basin was finally folded due to the closing of the back-arc basin (Fig. 14c). The orogen experienced a rapid uplift and erosion process at ca 800 Ma, fore-land molasses were formed, and an unconformity developed between the folded basement sequences and the overlying Neoproterozoic sequences. The eastern part of the Jiangnan orogen was uplifted to be a highland, and consequently post-orogenic extension started at ca 800–760 Ma (Fig. 14d). Significant upwelling of deep asthenospheric mantle and the collapse of the orogen took place at this stage. The upwelling of asthenosphere and the accompanying extension led to the partial melting of metasomatized lithospheric mantle formed during the earlier subduction. Therefore, the mafic rocks from the Shangshu and Puling Formations may exhibit arc-like geochemical features, but they were not formed in arc settings. The upwelling asthenosphere may also have melted to form OIB-like magmas. Meanwhile, the extension and the heating due to the elevation of temperature gradient may have lead to the partial melting of the crust. The partial melting of early Neoproterozoic juvenile crustal material produced the Xucun granitic porphyries and Shangshu rhyolites, while the melting of old crustal components led to the formation of the Puling felsic rocks.

8. Conclusions

The ca 800–760 Ma volcanic rocks in the eastern part of the Jiangnan orogen are commonly bimodal in composition. Both the metasomatized lithospheric mantle and the asthenosphere are considered as sources for the genesis of the mafic rocks. The metasomatized lithospheric mantle is the dominant source for most of the mafic rocks, whether their compositions are calc-alkaline or tholeiitic. The metasomatism may have been accomplished by the fluids or Na-rich melts from the subducted slab in early Neoproterozoic (ca 930–880 Ma) oceanic arc processes and the ca 870–840 Ma continental-arc processes. The partial melting of newly-metasomatized lithospheric mantle led to the formation of the mafic rocks in the Shangshu bimodal volcanics and the Puling mafic rocks. The high-degree partial melting of metasomatized lithospheric mantle led to the genesis of the Minjiawu mafic rocks of the Shangshu Formation. The partial melting of asthenosphere, plus possible crustal contamination or mixing with the metasomatized lithospheric mantle, led to the formation of the Xucun mafic rocks and some mafic rocks in the Shangshu Formation and Puling Formation. The eastern part of the Jiangnan orogen lacks geological evidence for plume activity, and the diversity of magma source requires post-orogenic extension for the genesis of the ca 800–760 Ma volcanic rocks.

Post-orogenic extension may have been diachronous along the whole Jiangnan orogen. It took place earlier in the eastern area but was more intense in the western parts. The Neoproterozoic within-plate rifting in South China, resulted from the post-orogenic extension, was closely related to the orogenic collapse of the Jiangnan orogen and there is no definite evidence to correlate it with the breakup of the Rodinia supercontinent. The eastern part of the Jiangnan orogen experienced a complex evolution, including subduction of oceanic crust and the formation of island arc magmatism at ca 930–880 Ma, arc-continent collision at ca 880–860 Ma, the closing of the back-arc basin at ca 860–800 Ma, and the final post-orogenic extension stage at ca 800–760 Ma.

Acknowledgements

This work was financially supported by the Ministry of Land and Resources of China (No. 200811015), the National Natural Science Foundation of China (No. 41072144), Department of Land and Resources of Zhejiang Province (2010001), and the MiDeR, NJU (2008-III-01). The manuscript benefited greatly from the constructive reviews of Profs. J. Charvet, and Q. Wang, and comments from the editor Prof. G.C. Zhao. We thank M.Q. Zhang for major element analysis, W. Pu for Sr-Nd isotopic analysis and H.J. Gong for CL imaging. W.L. Griffin kindly edited the English of the final version.

Appendix A. Supplementary data

Supplementary data associated with this article can be found, in the online version, at doi:10.1016/j.precamres.2011.07.003.

References

- Bai, W.J., Gan, Q.G., Yang, J.S., Xing, F.M., Xu, X., 1986. Discovery of well-reserved ophiolites and its basical characters in southeastern margin of the Jiangnan Ancient Continent. *Acta Petrol. Mineral.* 5 (4), 289–298 (in Chinese with English abstract).
- BGMRAP (Bureau of Geology and Mineral Resources of Hunan Province), 1987. Regional geology of Anhui Province. Geological Publishing House, Beijing, pp. 1–594 (in Chinese, with English Abstract).
- Blichert-Toft, J., Chauvel, C., Albarede, F., 1997. Separation of Hf and Lu for high-precision isotope analysis of rock samples by magnetic sector-multiple collector ICP-MS. *Contrib. Mineral. Petrol.* 127, 248–260.
- Bonin, B., Azzouni-Sekkal, A., Bussy, F., Ferrag, S., 1998. Alkali-calcic and alkaline post-orogenic (PO) granite magmatism: petrologic constraints and geodynamic settings. *Lithos* 45, 45–70.
- Bonin, B., 2004. Do coeval mafic and felsic magmas in post-collisional to within-plate regimes necessarily imply two contrasting, mantle and crustal, sources? A review. *Lithos* 78, 1–24.
- Burg, J.-P., Ford, M., 1997. Orogeny through time: an overview. *Geological Society, London, Special Publications* 121, 1–17.
- Charvet, J., Shu, L.S., Shi, Y.S., Guo, L.Z., Faure, M., 1996. The building of south China: collision of Yangzi and Cathaysia blocks, problems and tentative answers. *J. Southeast Asian Earth Sci.* 13 (3–5), 223–235.
- Chen, J.F., Foland, K.A., Xing, F.M., Xu, X., Zhou, T.X., 1991. Magmatism along the southeast margin of the Yangtze block: Precambrian collision of the Yangtze and Cathaysia blocks of China. *Geology* 19, 815–818.
- Chen, Z.H., Xing, G.F., Guo, K.Y., Dong, Y.G., Chen, R., Zeng, Y., Li, L.M., He, Z.Y., Zhao, L., 2009. Petrogenesis of keratophytes in the Pingshui Group, Zhejiang: constraints from zircon U-Pb ages and Hf isotopes. *Chin. Sci. Bull.* 54 (9), 1570–1578.
- Cheng, H., 1991. The late Proterozoic collision orogen in Northwestern Zhejiang Province. *Geol. Rev.* 37 (3), 203–213 (in Chinese, with English Abstract).
- Collins, W.J., 2002. Nature of extensional accretionary orogens. *Tectonics* 21 (4), doi:10.1029/2000TC001272.
- Davies, J.H., Blanckenburg, F.V., 1995. Slab breakoff: a model of lithosphere detachment and its test in the magmatism and deformation of collisional orogens. *Earth Planet. Sci. Lett.* 129, 85–102.
- Defant, M.J., Drummond, M.S., 1990. Derivation of some modern arc magmas by melting of young subducted lithosphere. *Nature* 367, 662–665.
- Dewey, J.F., 1988. Extensional collapse of orogens. *Tectonics* 7 (6), 1123–1139.
- Draut, A.E., Clift, P.D., Hannigan, R.E., Layne, G., Shimizu, N., 2002. A model for continental crust genesis by arc accretion: rare earth element evidence from the Irish Caledonides. *Earth Planet. Sci. Lett.* 203, 861–877.
- Eby, G.N., 1990. The A-type granitoids: a review of their occurrence and chemical characteristics and speculations on their petrogenesis. *Lithos* 26 (1–2), 115–134.
- Ernst, R.E., Buchan, K.L., Campbell, I.H., 2005. Frontiers in Large Igneous Province research. *Lithos* 79, 271–297.
- Gilbert, C.K., 1890. Lake Bonneville. US Geological Survey Monographs, 1.
- Griffin, W.L., Pearson, N.J., Elusiv, E., Jackson, S.E., van Achterberg, E., O'Reilly, S.Y., She, S.R., 2000. The Hf isotope composition of carbonic mantle: LAM-MC-ICPMS analysis of zircon megacrysts in kimberlites. *Geochim. Cosmochim. Acta* 64, 133–147.
- Guo, L.Z., Shi, Y.S., Ma, R.S., 1977. Discussion on the study methods of paleo-trench-arc system and their implications. *Fujian Geol.* (4), 1–24 (in Chinese with English abstract).
- Hu, J., Qiu, J.S., Xu, X.S., Wang, X.L., Li, Z., 2010. Geochronology and geochemistry of gneissic metagranites in eastern Dabie Mountains: implications for the Neoproterozoic tectono-magmatism along the northeastern margin of the Yangtze Block. *Sci. Chin. (Earth Sci.)* 53 (4), 501–517.
- Huang, X.-L., Xu, Y.-G., Li, X.-H., Li, W.-X., Lan, J.-B., Zhang, H.-H., Liu, Y.-S., Wang, Y.-B., Li, H.-Y., Luo, Z.-Y., Yang, Q.-J., 2008. Petrogenesis and tectonic implications of Neoproterozoic, highly fractionated A-type granites from Mianning, South China Original Research Article. *Precamb. Res.* 165, 190–204.

- Hyndman, R.D., Currie, C.A., Mazzotti, S.P., 2005. Subduction zone backarcs, mobile belts, and orogenic heat. *GSA Today* 15 (2), 1–10.
- Irvine, T.N., Baragar, W.R., 1971. A guide to the chemical classification of the common volcanic rocks. *Can. J. Earth Sci.* 8, 523–548.
- JPIGS (Jiangxi Provincial Institute of Geological Survey), 2006. Regional Geological Survey Report (Shangrao area, 1:250,000) (in Chinese with English Abstract).
- JPIGS (Jiangxi Provincial Institute of Geological Survey), 2007. Regional Geological Survey Report (Jingdezhen area, 1:250,000) (in Chinese with English Abstract).
- Kellemen, P.B., Hanghøj, K., 2004. One view of the geochemistry of subduction-related magmatic arcs, with an emphasis on primitive andesite and lower crust. In: Rudnick, R.L. (Ed.), *The Crust: Treatise on Geochemistry*, vol. 3, pp. 593–659.
- Lesher, C.E., 1990. Decoupling of chemical and isotopic exchange during magma mixing. *Nature* 344 (15), 235–237.
- Li, Z.-X., Zhang, L.H., Powell, C.M.C., 1995. South China in Rodinia: part of the missing link between Australia-East Antarctica and Laurentia? *Geology* 23 (5), 407–410.
- Li, Z.X., Li, X.H., Kinny, P.D., Wang, J., 1999. The breakup of Rodinia: did it start with a mantle plume beneath South China? *Earth Planet. Sci. Lett.* 173, 171–181.
- Li, X.H., Li, Z.X., Ge, W.C., Zhou, H.W., Li, W.X., Liu, Y., Wingate, M.T.D., 2003a. Neoproterozoic granitoids in South China: crustal melting above a mantle plume at ca. 825 Ma? *Precamb. Res.* 122, 45–83.
- Li, Z.X., Li, X.H., Kinny, P.D., Wang, J., Zhang, S., Zhou, H.W., 2003b. Geochronology of Neoproterozoic syn-rift magmatism in the Yangtze Craton, South China and correlations with other continents: evidence for a mantle superplume that broke up Rodinia. *Precamb. Res.* 122, 85–109.
- Li, X.-H., Li, Z.-X., Sinclair, J.A., Li, W.-X., Carter, G., 2007. Understanding dual geochemical characters in a geological context for the Gaojiacun intrusion: Response to Munteanu and Yao's discussion [Precamb. Res. 154 (2007) 164–167]. *Precamb. Res.* 155, 328–332.
- Li, W.X., Li, X.H., Li, Z.X., 2008a. Middle Neoproterozoic syn-rifting volcanic rocks in Guangfeng, South China: petrogenesis and tectonic significance. *Geol. Mag.* 145 (4), 475–489.
- Li, X.-H., Li, W.-X., Li, Z.-X., Liu, Y., 2008b. 850–790 Ma bimodal volcanic and intrusive rocks in northern Zhejiang, South China: a major episode of continental rift magmatism during the breakup of Rodinia. *Lithos* 102, 341–357.
- Li, X.-H., Li, W.-X., Li, Z.-X., Lo, C.-H., Wang, J., Ye, M.-F., Yang, Y.-H., 2009. Amalgamation between the Yangtze and Cathaysia Blocks in South China: Constraints from SHRIMP U-Pb zircon ages, geochemistry and Nd-Hf isotopes of the Shuangxiwu volcanic rocks. *Precamb. Res.* 174, 117–128.
- Ma, L.F., Qiao, X.F., Min, L.R., Fan, B.X., Ding, X.Z., 2002. Chinese geological illustrated handbook, pp. 245–252. Beijing: Geological Publishing House.
- Ma, R.S., Yu, X.Q., Cheng, G.H., 2001. On the Dengjia and Puling formations in south Anhui. *Geol. Anhui* 11 (2), 95–105 (in Chinese with English abstract).
- Maitre, R.W.L., Bateman, P., Dudek, A., Keller, J., Lemeyre, J., Bas, M.J.L., Sabine, P.A., Schmid, R., Sorensen, H., Streckeisen, A., Wooley, A.R., Zanettin, B., 1989. A Classification of Igneous Rocks and Glossary of Terms. Blackwell, Oxford.
- Maniar, P.D., Piccoli, P.M., 1989. Tectonic discrimination of granitoids. *Geol. Soc. Am. Bull.* 101 (5), 635–643.
- Nowell, G.M., Kempton, P.D., Noble, S.R., Fitton, J.G., Saunders, A.D., Mahoney, J.J., Taylor, R.N., 1998. High precision Hf isotope measurements of MORB and OIB by thermal ionisation mass spectrometry: insights into the depleted mantle. *Chem. Geol.* 149, 211–233.
- Pu, W., Gao, J.F., Zhao, K.D., Ling, H.F., Jiang, S.Y., 2005. Separation method of Rb-Sr, Sm-Nd using DCTA and HIBA. *J. Nanjing Univ. (Nat. Sci.)* 41 (4), 445–450 (in Chinese with English Abstract).
- Scherer, E., Munker, C., Mezger, K., 2001. Calibration of the lutetium-hafnium clock. *Science* 293, 683–687.
- Sheth, H.C., 2007. 'Large Igneous Provinces (LIPs)': definition, recommended terminology, and a hierarchical classification. *Earth-Sci. Rev.* 85, 117–124.
- Shu, L.S., Shi, Y.S., Gou, L.Z., Charvet, J., Sun, Y. (Eds.), 1995. Plate Tectonic Evolution and the Kinematics of Collisional Orogeny in the Middle Jiangnan, Eastern China. Nanjing University Publ., p. 174 (in Chinese with English Abstract).
- Shu, L., Charvet, J., 1996. Kinematics and geochronology of the Proterozoic Dongxiang-Shexian ductile shear zone: with HP metamorphism and ophiolitic mélange (Jiangnan region, South China). *Tectonophysics* 267, 291–302.
- Shui, T., Xu, B.T., Liang, R.H., Qiu, Y.S., 1986. Shaoxing-Jianguo deep-seated fault zone, Zhejiang Province. *Chin. Sci. Bull.* 31 (18), 1250.
- Sun, S.S., McDonough, W.F., 1989. Chemical and isotopic systematics of oceanic basalt: implications for mantle composition and processes. In: Saunders, A.D., Norry, M.J. (Eds.), *Magmatism in the Ocean Basins: Geological Society [London] Special Publications* 42, pp. 313–345.
- Tang, H.F., Zhou, X.M., Zhi, L.G., 1997. Discovery and significance of Xucun late Proterozoic composite dike swarm in southern Anhui Province. *Chin. Sci. Bull.* 42 (4), 328.
- Teixeira, W., Pineiro, J.P.P., Iacumin, M., Girardi, V.A.V., Piccirillo, E.M., Echeveste, H., Ribot, A., Fernandez, R., Renne, P.R., Heaman, L.M., 2002. Calc-alkaline and tholeiitic dyke swarms of Tandilia, Rio de la Plata craton, Argentina: U-Pb, Sm-Nd, and Rb-Sr $^{40}\text{Ar}/^{39}\text{Ar}$ data provide new clues for intraplate rifting shortly after the Trans-Amazonian orogeny. *Precamb. Res.* 119, 329–353.
- Vervoort, J.D., Patchett, P.J., Soderlund, U., Baker, M., 2004. Isotopic composition of Yb and the determination of Lu concentrations and Lu/Hf ratios by isotopic dilution using MC-ICPMS. *Geochem. Geophys. Geosys.* 5, 2004GC000721.
- Wang, J., Li, Z.X., 2003. History of Neoproterozoic rift basins in South China: implications for Rodinia break-up. *Precamb. Res.* 122, 141–158.
- Wang, X.L., Zhou, J.C., Qiu, J.S., Gao, J.F., 2004. Geochemistry of the Meso- to Neoproterozoic basic-acid rocks from Hunan Province, South China: implications for the evolution of the western Jiangnan orogen. *Precamb. Res.* 135, 79–103.
- Wang, X.L., Zhou, J.C., Qiu, J.S., Zhang, W.L., Liu, X.M., Zhang, G.L., 2006. LA-ICP-MS U-Pb zircon geochronology of the Neoproterozoic igneous rocks from Northern Guangxi, South China: implications for petrogenesis and tectonic evolution. *Precamb. Res.* 145 (1–2), 111–130.
- Wang, X.L., Zhou, J.C., Griffin, W.L., Wang, R.C., Qiu, J.S., O'Reilly, S.Y., Xu, X.S., Liu, X.M., Zhang, G.L., 2007. Detrital zircon geochronology of Precambrian basement sequences in the Jiangnan orogen: dating the assembly of the Yangtze and Cathaysia blocks. *Precamb. Res.* 159 (1–2), 117–131.
- Wang, X.L., Zhou, J.C., Qiu, J.S., Jiang, S.Y., Shi, Y.R., 2008a. Geochronology and geochemistry of Neoproterozoic mafic rocks from western Hunan, South China: implications for petrogenesis and post-orogenic extension. *Geol. Mag.* 145 (2), 215–233.
- Wang, X.L., Zhao, G.C., Zhou, J.C., Liu, Y.S., Hu, J., 2008b. Geochronology and Hf isotopes of zircon from volcanic rocks of the Shuangqiaoshan Group, South China: implications for the Neoproterozoic tectonic evolution of the eastern Jiangnan orogen. *Gondwana Res.* 14 (3), 355–367.
- Wang, X.L., Jiang, S.Y., Dai, B.Z., 2010a. Melting of enriched Archean subcontinental lithospheric mantle: Evidence from the ca. 1760 Ma volcanic rocks of the Xiong'er Group, southern margin of the North China Craton. *Precamb. Res.* 182, 204–216.
- Wang, Q., Wyman, D.A., Li, Z.-X., Bao, Z.-W., Zhao, Z.-H., Wang, Y.-X., Jian, P., Yang, Y.-H., Chen, L.-L., 2010b. Petrology, geochronology and geochemistry of ca. 780 Ma A-type granites in South China: Petrogenesis and implications for crustal growth during the breakup of the supercontinent Rodinia. *Precamb. Res.* 178, 185–208.
- Wang, L.J., Griffin, W.L., Yu, J.H., O'Reilly, S.Y. et al., 2010c. Precambrian crustal evolution of the Yangtze Block tracked by detrital zircons from Neoproterozoic sedimentary rocks. *Precamb. Res.* 177, 131–144.
- Wilson, J.T., 1966. Did the Atlantic close and then re-open? *Nature* 211, 676–681.
- Winchester, J.A., Floyd, P.A., 1977. Geochemical discrimination of different magma series and their differentiation products. *Chem. Geol.* 20, 325–343.
- Wu, F.Y., Yang, Y.H., Xie, L.W., Yang, J.H., Xu, P., 2006a. Hf isotopic compositions of the standard zircons and baddeleyites used in U-Pb geochronology. *Chem. Geol.* 234, 105–126.
- Wu, R.X., Zheng, Y.F., Wu, Y.B., Zhao, Z.F., Zhang, S.B., Liu, X.M., Wu, F.Y., 2006b. Reworking of juvenile crust: element and isotope evidence from Neoproterozoic granodiorite in South China. *Precamb. Res.* 146, 179–212.
- Yu, J.-H., O'Reilly, S.Y., Wang, L.J., Griffin, W.L., Zhang, M., Wang, R.C., Jiang, S.Y., Shu, L.S., 2008. Where was South China in the Rodinia supercontinent? Evidence from U-Pb geochronology and Hf isotopes of detrital zircons. *Precamb. Res.* 164, 1–15.
- Yu, J.-H., Wang, L.J., O'Reilly, S.Y., Griffin, W.L., Zhang, M., Li, C.Z., Shu, L.S., 2009. A Paleoproterozoic orogeny recorded in a long-lived cratonic remnant (Wuyishan terrane), eastern Cathaysia Block, China. *Precamb. Res.* 174, 347–363.
- Yu, J.H., O'Reilly, S.Y., Wang, L.J., Griffin, W.L., Zhou, M.F., Zhang, M., Shu, L.S., 2010. Components and episodic growth of Precambrian crust in the Cathaysia Block, South China: evidence from U-Pb ages and Hf isotopes of zircons in Neoproterozoic sediments. *Precamb. Res.* 181, 97–114.
- Zhao, G.C., Cawood, P.A., 1999. Tectonothermal evolution of the Mayuan assemblage in the Cathaysia Block: new evidence for Neoproterozoic collisional-related assembly of the South China craton. *Am. J. Sci.* 299, 309–339.
- Zhao, J.-H., Zhou, M.-F., Yan, D.-P., Zheng, J.-P., Li, J.-W., 2011. Reappraisal of the ages of Neoproterozoic strata in South China: no connection with the Grenvillian orogeny. *Geology* 39, 299–302.
- Zhao, X.F., Zhou, M.F., Li, J.W., Sun, M., Gao, J.F., Sun, W.H., Yang, J.H., 2010. Late Paleoproterozoic to early Mesoproterozoic Dongchuan Group in Yunnan, SW China: implications for tectonic evolution of the Yangtze Block. *Precamb. Res.* 182, 57–69.
- Zheng, Y.F., Zhang, S.B., Zhao, Z.-F., Wu, Y.B., Li, X.H., Li, Z.X., Wu, F.-Y., 2007. Contrasting zircon Hf and O isotopes in the two episodes of Neoproterozoic granitoids in South China: implications for growth and reworking of continental crust. *Lithos* 96, 127–150.
- Zheng, Y.F., Wu, R.X., Wu, Y.B., Zhang, S.B., Yuan, H.L., Wu, F.Y., 2008. Rift melting of juvenile arc-derived crust: geochemical evidence from Neoproterozoic volcanic and granitic rocks in the Jiangnan Orogen, South China. *Precamb. Res.* 163, 351–383.
- Zhou, M.F., Yan, D.P., Kennedy, A., Li, Y.Q., Ding, J., 2002. SHRIMP U-Pb zircon geochronological and geochemical evidence for Neoproterozoic arc-magmatism along the western margin of the Yangtze Block, South China. *Earth Planet. Sci. Lett.* 196, 51–67.
- Zhou, J.C., Wang, X.L., Qiu, J.S., Gao, J.F., 2004. Geochemistry of Meso- and Neoproterozoic mafic-ultramafic rocks from northern Guangxi, China: arc or plume magmatism? *Geochim. J.* 38, 139–152.
- Zhou, X.M., Sun, T., Shen, W.Z., Shu, L.S., Niu, Y.L., 2006a. Petrogenesis of Mesozoic granitoids and volcanic rocks in South China: a response to tectonic evolution. *Episodes* 29 (1), 26–33.

- Zhou, M.F., Yan, D.P., Wang, C.L., Qi, L., Kennedy, A., 2006b. Subduction-related origin of the 750 Ma Xuelongbao adakitic complex (Sichuan Province, China): Implications for the tectonic setting of the giant Neoproterozoic magmatic event in South China. *Earth Planet. Sci. Lett.* 248, 286–300.
- Zhou, J.C., Wang, X.L., Qiu, J.S., 2009. Geochronology of Neoproterozoic mafic rocks and sandstones from northeastern Guizhou, South China: Coeval arc magmatism and sedimentation. *Precamb. Res.* 170, 27–42.
- Zhou, X.M., Wang, D.Z., 1988. The peraluminous granodiorites with low initial $^{87}\text{Sr}/^{86}\text{Sr}$ ratio and their genesis in southern Anhui Province, eastern China. *Acta Petrol. Sin.* 4, 37–45 (in Chinese with English abstract).
- Zhou, X.M., 2003. My thinking about granite geneses of South China. *Geol. J. Chin. Univ.* 9 (4), 556–565 (in Chinese with English abstract).
- Zhou, X.M., Zhu, Y.H., 1993. Late Proterozoic Collisional orogen and geosuture in Southeastern China: petrological evidence. *Chin. J. Geochem.* 12 (3), 239–251.